cmgh
CELLULAR AND MOLECULAR GASTROENTEROLOGY AND HEPATOLOGY

ORIGINAL RESEARCH

# BMSCs Promote Differentiation of Enteric Neural Precursor Cells to Maintain Neuronal Homeostasis in Mice With Enteric Nerve Injury

Mengke Fan,* Huiying Shi,* Hailing Yao, Weijun Wang, Yurui Zhang, Chen Jiang, and Rong Lin

*Department of Gastroenterology, Union Hospital, Tongji Medical College, Huazhong University of Science and Technology, Wuhan, China*

## SUMMARY

In enteric nerve injury cases, ENPCs differentiate into enteric neurons and glial cells promoting ENS repair and gastric motility recovery after BMSCs transplantation. A small number of BMSCs located in the myenteric plexus differentiate into glial cells expressing high level GDNF. GDNF secreted by BMSCs promotes the proliferation and differentiation of ENPCs in vitro.

**BACKGROUND & AIMS:** Our previous study showed that transplantation of bone marrow–derived mesenchymal stem cells (BMSCs) promoted functional enteric nerve regeneration in denervated mice but not through direct transdifferentiation. Homeostasis of the adult enteric nervous system (ENS) is maintained by enteric neural precursor cells (ENPCs). Whether ENPCs are a source of regenerated nerves in denervated mice remains unknown.

**METHODS:** Genetically engineered mice were used as recipients, and ENPCs were traced during enteric nerve regeneration. The mice were treated with benzalkonium chloride to establish a denervation model and then transplanted with BMSCs 3 days later. After 28 days, the gastric motility and ENS regeneration were analyzed. The interaction between BMSCs and ENPCs in vitro was further assessed.

**RESULTS:** Twenty-eight days after transplantation, gastric motility recovery (gastric emptying capacity, $P < .01$; gastric contractility, $P < .01$) and ENS regeneration (neurons, $P < .01$; glial cells, $P < .001$) were promoted in BMSCs transplantation groups compared with non-transplanted groups in denervated mice. More importantly, we found that ENPCs could differentiate into enteric neurons and glial cells in denervated mice after BMSCs transplantation, and the proportion of $Nestin^+$/$Ngfr^+$ cells differentiated into neurons was significantly higher than that of $Nestin^+$ cells. A small number of BMSCs located in the myenteric plexus differentiated into glial cells. In vitro, glial cell–derived neurotrophic factor (GDNF) from BMSCs promotes the migration, proliferation, and differentiation of ENPCs.

**CONCLUSIONS:** In the case of enteric nerve injury, ENPCs can differentiate into enteric neurons and glial cells to promote ENS repair and gastric motility recovery after BMSCs transplantation. BMSCs expressing GDNF enhance the migration, proliferation, and differentiation of ENPCs. *(Cell Mol Gastroenterol Hepatol 2023;15:511–531; https://doi.org/10.1016/j.jcmgh.2022.10.018)*

*Keywords:* Bone Marrow-Derived Mesenchymal Stem Cells; Enteric Neural Precursor Cells; Glial Cell-Derived Neurotrophic Factor; Enteric Nervous System.

The enteric nervous system (ENS), an independent network of enteric neurons and glial cells, plays an important role in the regulation of gastrointestinal physiology.[1,2] ENS injuries and degeneration are significant pathogenic factors in gastrointestinal motility disorders, including esophageal achalasia and gastroparesis.[3,4] However, currently available therapeutic options are far from satisfactory, such as surgical resection and medical management (support or nutrition).[5,6] Stem cell transplantation shows great potential for inducing compensatory nerve regeneration and recovery of gastrointestinal motility.[7–9]

In recent years, bone marrow–derived mesenchymal stem cells (BMSCs) have emerged as promising candidates for the treatment of tissue damage and neurodegenerative disorders.[10–14] Their unique advantages include ease of isolation, proliferation[11,15] and immune pardon after transplantation.[16–18] Our previous study indicated that BMSCs transplantation promotes ENS remodeling and restores muscle contractility in rats with pylorus denervation. However, the regenerated neurons were not derived from transplanted

*Authors share co-first authorship.

***Abbreviations used in this paper:*** **α-SMA, alpha smooth muscle actin; BAC, benzalkonium chloride; bFGF, basic fibroblast growth factor; BMSCs, bone marrow–derived mesenchymal stem cells; DAPI, 4,6-diamidino-2-phenylindole; DT, diphtheria toxin; EdU, 5-ethynyl-2′-deoxyuridine; EFS, electric field stimulation; EGF, epidermal growth factor; ENPCs, enteric neural precursor cells; ENS, enteric nervous system; E16-18, embryonic period 16-18 days; FGF, fibroblast growth factor; GDNF, glial cell-derived neurotrophic factor; GFAP, glial fibrillary acidic protein; GFP, green fluorescent protein; IL, interleukin; LM-MP, longitudinal muscle-myenteric plexus; Ngfr/p75, nerve growth factor receptor; nNOS, neuronal nitric oxide synthase; PBS, phosphate-buffered saline; PGP 9.5, protein gene product 9.5; RET, RET proto-oncogene; SiRNA, small interfering RNA; SOX10, sex determining region Y-box10 protein; TAM, tamoxifen.**

Most current article


2352-345X
https://doi.org/10.1016/j.jcmgh.2022.10.018

BMSCs.[19] The source of the regenerated neurons in ENS-injured mice after BMSCs transplantation is unclear.

Previous studies have confirmed that enteric neural precursor cells (ENPCs) maintain ENS homeostasis in healthy adult mice.[20,21] ENPCs are capable of neurogenesis in vivo in healthy adult gut. However, whether ENPCs generate the neuronal and glial lineages of enteric ganglia to maintain neuronal homeostasis in denervated mice has not yet been studied. In addition, there are no markers that specifically label the ENPCs in postnatal intestine because the identity of these cells is unknown. Previous studies identified ENPCs using Nestin, which is expressed by a variety of neural stem cells.[22–24] The nerve growth factor receptor (Ngfr/p75) is expressed in many cell types. Kulkarni et al[20] found that only $Nestin^+/Ngfr^+$ cells in myenteric express stem cell behaviors in vitro, and $Nestin^+/Ngfr^+$ may be the special markers for ENPCs. To explore the fate of $Nestin^+$ and $Nestin^+/Ngfr^+$ cells during enteric nerve regeneration in denervated mice, we used a double-transgenic mouse strain (Nestin-creERT2: tdTomato) and a triple-transgenic mouse strain (Nestin-creert2 × Ngfr-Dreert2: DTRGFP) in this study.

As a neuron protective factor, glial cell–derived neurotrophic factor (GDNF) is essential for survival, proliferation, and migration of ENS progenitors and the development of ENS.[25,26] Soret et al[27] reported that GDNF treatment using rectal enemas induces enteric neurogenesis and improves colonic structure and function in mouse models of Hirschsprung disease. Interestingly, our previous study found that the protein expression of GDNF in BMSCs was significantly up-regulated after preconditioning with exogenous GDNF in vitro. In addition, BMSCs transplantation group showed a stable high level of GDNF expression in denervated pyloric wall compared with the denervated group in vivo.[19] However, the mechanism by which GDNF derived from BMSCs promotes enteric neurogenesis in mice with ENS injury remains unclear.

The aim of this study was to investigate the fate of ENPCs during enteric nerve regeneration in ENS-injured mice and to clarify the mechanism by which BMSCs promote enteric nerve regeneration.

## Results

### *Stable Denervated Mice Were Successfully Established*

Immunofluorescence analysis showed that the neural clusters labeled with protein gene product (PGP) 9.5/HuC/D/glial fibrillary acidic protein (GFAP) were completely and regularly arranged in the control group (Figure 1*A*–*D*). No neuronal (PGP 9.5, HuC/D; Figure 1*A*–*C*) and glial (GFAP; Figure 1*D*) markers were found in the benzalkonium chloride (BAC)-treated region at 31 days after surgery. Moreover, Western blot analyses confirmed that BAC treatment significantly down-regulated the expression of neuronal (PGP9.5, HuC/D) and glial (GFAP) markers (Figure 1*E* and *F*, $P < .0001$). These results indicated that the gastric denervation model was successfully established.

### *BMSCs Expressing Glial Cell Characteristic Protein Promoted Gastrointestinal Nerve Regeneration in Denervated Mice*

In BMSCs subjected to precondition before transplantation, the result indicated that the expression of neurotrophic factor genes (GDNF, $P < .0001$; BDNF, $P < .01$), anti-inflammatory factor gene (interleukin [IL] 13, $P < .05$), and anti-apoptosis related genes (Survivin, $P < .0001$) of BMSCs were significantly increased after preconditioning (Figure 2). The gene expression level of GDNF in BMSCs with precondition was 3 times higher than untreated, and the protein expression levels of glial cell characteristic markers (GFAP, $P < .05$; GDNF, $P < .001$) were significantly up-regulated after preconditioning (Figure 3*A* and *B*). In vivo, the preconditioned green fluorescent protein (GFP)/tdTomato-labeled BMSCs were transplanted into the stomach of mice, and their distribution was tracked (Figure 3*C*). One day after transplantation, immunofluorescence microscopy showed that BMSCs survived and distributed in the subserosal/muscular layer. At 3 days after transplantation, laser confocal immunofluorescence microscopy showed that most BMSCs had migrated to the submucosa. At 28 days after transplantation, most of the BMSCs were distributed in the submucosa, and a few were distributed in the muscular/mucosal layer. To further elucidate the specific role of BMSCs, we analyzed the co-localization of tdTomato-labeled BMSCs with the expression of the glial cell marker GFAP or the neuron marker β-tubulin (Figure 3*D*). Immunofluorescence microscopy revealed glial cells in the myenteric plexus are labeled with tdTomato, indicating their originates from the BMSCs. However, neurons are not labeled with tdTomato.

The BAC model was used to determine whether BMSCs transplantation promoted ENS regeneration (Figure 3*E*). Immunofluorescence results showed neural clusters labeled with β-tubulin/GFAP were completely and regularly arranged in the control/sham group. However, no glial cells (GFAP) and neurons (β-tubulin) were found in the BAC group. Then the treated area was colonized by glial cells and neuron in the BAC + BMSCs group 28 days after transplantation. Similarly, the protein expression of neuronal markers (HuC/D, $P < .001$; β-tubulin, $P < .01$) and glial markers (GFAP, $P < .001$) was significantly up-regulated in the BMSCs transplanted group compared with the BAC group (Figure 3*F*). In addition, BMSCs transplantation up-regulated the expression level of GDNF/BDNF gene in denervated mice ($P < .01$; Figure 4). In addition, BMSCs transplantation reduced the level of inflammatory cytokine (IL-6, $P < .001$) and increased the level of anti-inflammatory cytokine (IL-13, $P < .05$) and anti-apoptosis related genes (Survivin, $P < .05$) in BAC mice. These results indicated that BMSCs function as glial cells effectively promoted ENS remodeling in denervated mice.

### *BMSCs Transplantation Promoted Gastric Motility Recovery (Gastric Emptying Capacity and Contractility) in Denervated Mice*

Twenty minutes after the administration of the test meal, the gastric tissues in the different groups were visually

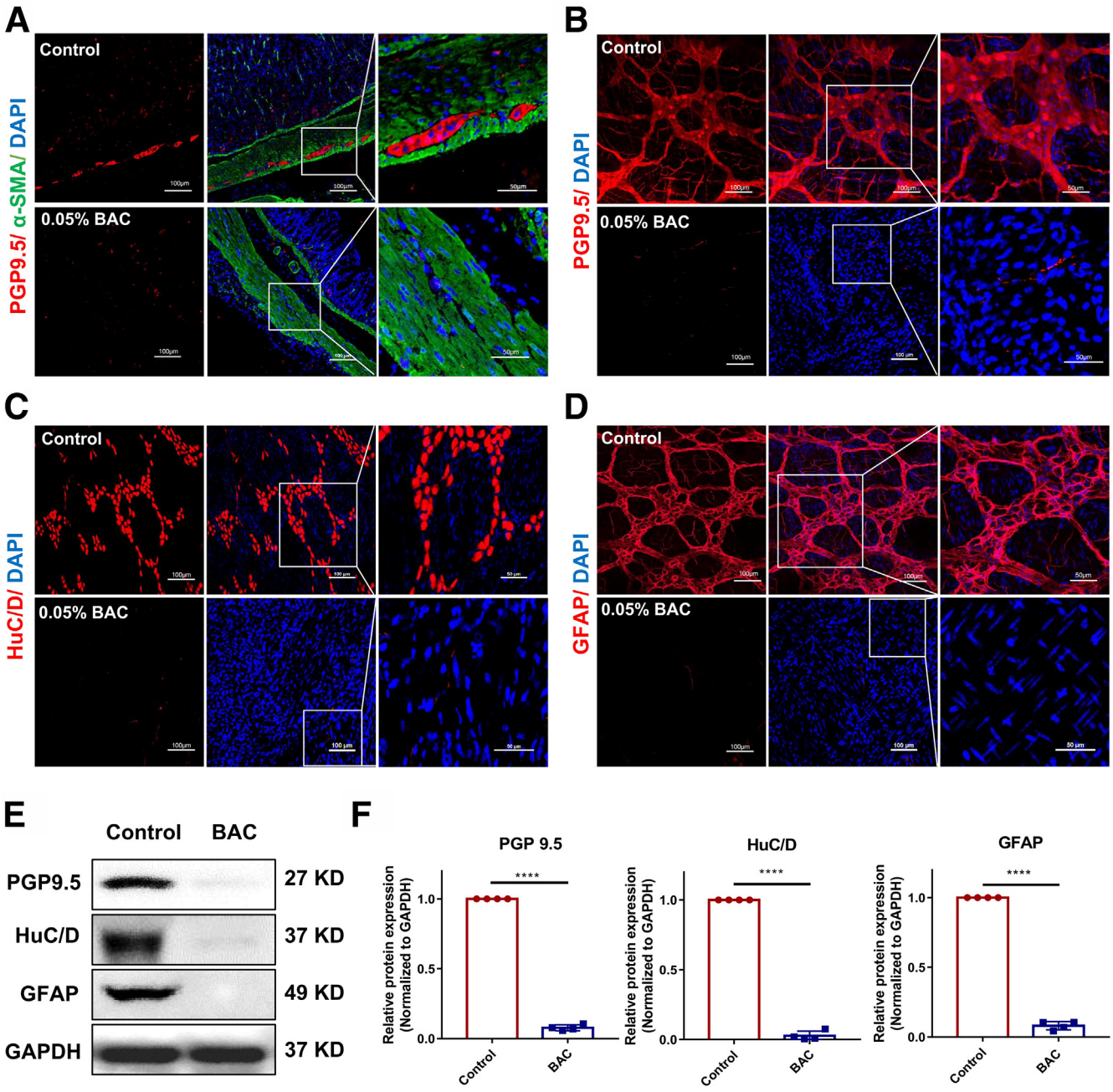


**Figure 1. BAC (0.05%) effectively ablated the myenteric plexus in gastric tissue and remained at least 31 days.** *(A)* Representative immunofluorescence confocal laser images in transverse sections of gastric tissue sections of PGP 9.5 (*red*) in the control group (*upper panel*) and 0.05% BAC treated group (*lower panel*); the α-SMA (*green*); the nuclei (*blue*). *(B–D)* Representative immunofluorescence confocal laser images in gastric myenteric plexus of PGP 9.5 (*red*), HuC/D (*red*), and GFAP (*red*) in each group; the nuclei (*blue*). *(E* and *F)* Representative immunoblot bands and histogram of relative expression for PGP 9.5/HuC/D/GFAP in each group (normalized to GAPDH). Control, the control C57 mice; BAC, benzalkonium chloride treated C57 mice. Results were expressed as mean ± standard deviation. $^{****}P < .0001$, n = 4–5.

observed, and the results are shown in Figure 5*A*. There was no significant difference in gastric motility between control and sham groups. However, liquid gastric emptying at 20 minutes was delayed in the BAC group compared with that in the control group ($P < .0001$). Gastric emptying was significantly accelerated in mice that received BMSCs transplantation compared with that in the BAC group ($P < .01$; Figure 5*A* and *B*). In addition, the results of stomach weight analysis were consistent with those of gastric emptying (Figure 5*C*).

In addition, spontaneous contractions (Figure 5*D*) and contractile responses of gastric muscle strips induced by electric field stimulation (EFS) (Figure 5*G*) were evaluated. The gastric muscle strips of the BAC group displayed lower

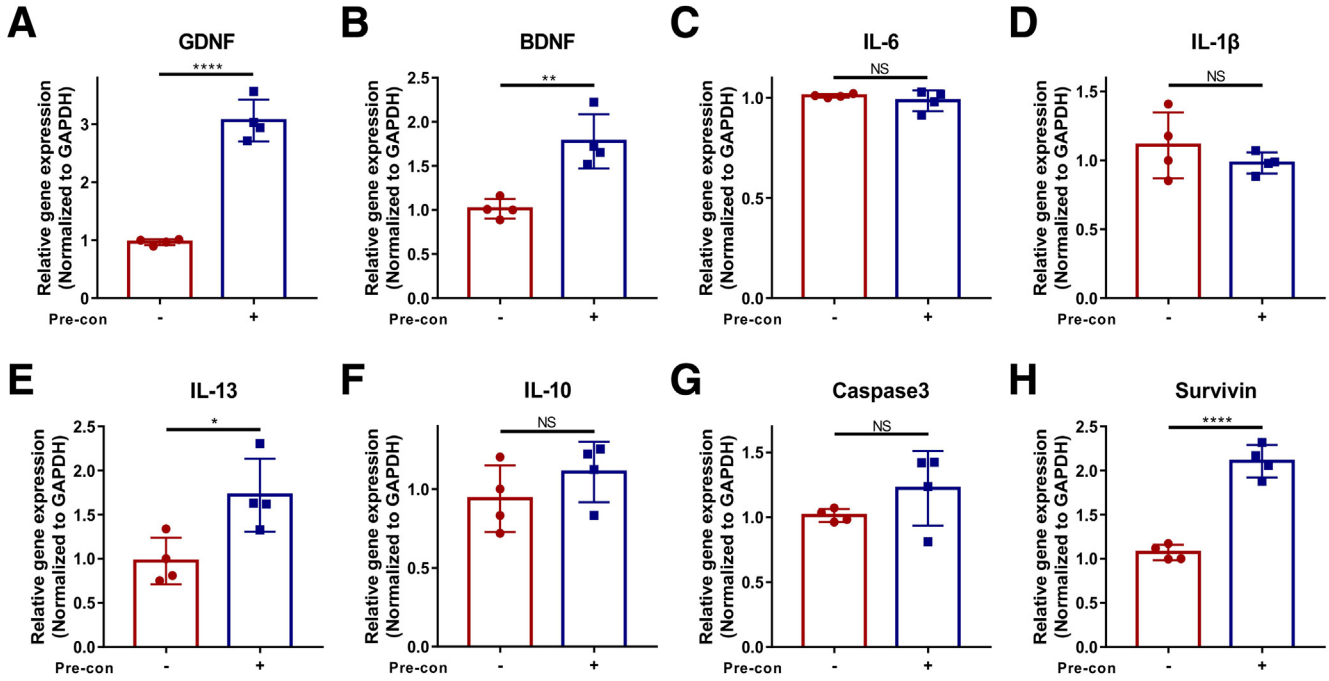


**Figure 2. Genes associated with neurotrophic factor, anti-inflammatory factor, and anti-apoptosis factor of BMSCs were significantly up-regulated after precondition.** *(A* and *B)* Transcripts of neurotrophic factor genes (GDNF/BDNF), *(C* and *D)* inflammatory cytokines genes (IL-6/IL-1$\beta$), *(E* and *F)* anti-inflammatory genes (IL-10/IL-13), and *(G* and *H)* apoptosis-related genes (Caspase 3, Survivin) of BMSCs in different groups were determined by reverse transcriptase polymerase chain reaction assay. Results were expressed as mean ± standard deviation. $^{*}P < .05$, $^{**}P < .01$, $^{****}P < .0001$, NS, no significance.

contraction frequency ($P < .001$; Figure 5*E*) and higher contraction amplitude ($P < .05$; Figure 5*F*) than those of the control group. Moreover, BMSCs transplantation significantly restored the spontaneous contractility of gastric muscle strips ($P < .01$; Figure 5*E* and *F*). In addition, the contractile response of the gastric muscle strips induced by EFS was severely impaired in the BAC group. BMSCs transplantation showed a significant restorative effect on EFS-induced contractions in BAC + BMSCs group ($P < .01$; Figure 5*H*).

## *Nestin$^+$ Cells Differentiated Into Neurons and Glial Cells in Denervated Mice (Nestin-creERT2: tdTomato Mice)*

Nestin-creERT2: tdTomato mice were used to track the Nestin$^+$ cells in vivo. In the control, myenteric plexus was regularly arranged, and no tdTomato-labeled Nestin$^+$ cells were detected (Figure 6*A*). In the control + tamoxifen (TAM) and sham + TAM groups, some neurons ($\beta$-tubulin, HuC/D, and neuronal nitric oxide synthase [nNOS]) and glial (GFAP) cells are labeled with tdTomato, indicating their origin from the Nestin$^+$ cells (Figure 6*B* and *C*). In the BAC group, no neurons and glial cells were found, and the number of Nestin$^+$ cells significantly decreased compared with the control (Figure 6*D*).

To determine the roles of Nestin$^+$ cells and BMSCs in nerve regeneration, we performed triple immunofluorescence staining in freshly harvested myenteric plexus tissues: tdTomato-labeled Nestin$^+$ cells (red), GFP-labeled BMSCs (green), and neuronal/glial markers (gray) (Figure 6*E* and *F*). At 28 days after transplantation, regenerated neurons and glial cells were detected in the BAC + BMSCs + TAM group. The Nestin$^+$ cells express neuronal markers ($\beta$-tubulin, HuC/D, and nNOS) or glial markers (GFAP), and the transplanted BMSCs express glial marker (GFAP) (Figure 6*F*). These results indicated that a population of Nestin$^+$ cells differentiated into enteric neurons and glial cells after BMSCs transplantation in mice with gastric denervation.

## *Nestin$^+$/Ngfr$^+$ Cells Differentiated Into Neurons and Glial cells in Denervated Mice (Nestin-creert2 × Ngfr-Dreert2: DTRGFP Mice)*

Nestin-creert2 × Ngfr-Dreert2: DTRGFP mice were used to track Nestin$^+$/Ngfr$^+$ cells in vivo. In the control, the nerve clusters were neatly arranged, and no GFP-labeled Nestin$^+$/Ngfr$^+$ cells were detected (Figure 7*A*). In the control + TAM and sham + TAM groups, co-expression of GFP and neuronal/glial markers confirmed some neurons and glial origin from the Nestin$^+$/Ngfr$^+$ cells in adult mice (Figure 7*B* and *C*). In the BAC group, no neuron/glial were found in the BAC-treated region, and Nestin$^+$/Ngfr$^+$ cells decreased compared with the control group (Figure 7*D*).

To track the fate of Nestin$^+$/Ngfr$^+$ cells and BMSCs, triple immunofluorescence staining of GFP-labeled Nestin$^+$/Ngfr$^+$ cells (green), tdTomato-labeled BMSCs (red), and neuronal markers/glial markers (gray) was performed (Figure 7*E* and *F*). About 28 days later, the treated area was

colonized by regenerated neurons and glial cells in the BAC + BMSCs + TAM group. The regenerated glial cells (GFAP) in the myenteric plexus are labeled with GFP or tdTomato, indicating their origin from the Nestin$^+$/Ngfr$^+$ cells or BMSCs. The regenerated neuronas ($\beta$-tubulin/HuC/D/nNOS) are labeled with GFP, indicating their origin from the Nestin$^+$/Ngfr$^+$ cells (Figure 7*F*).

### *The Proportion of Nestin$^+$/Ngfr$^+$ Cells Differentiated Into Neurons Was Significantly Higher Than That of Nestin$^+$ Cells*

The proportion of Nestin$^+$ and Nestin$^+$Ngfr$^+$ cells that differentiated into neurons and glial cells on day 28 was further evaluated: (1) Nestin-creERT2: tdTomato mice, tdTomato-labeled Nestin$^+$ cells (red), and neuronal markers/glial markers (green) (Figures 6*B* and 8*A*); (2) Nestin-creert2 × Ngfr-Dreert2: DTRGFP mice, GFP-labeled Nestin$^+$/Ngfr$^+$ cells (green) and neuronal markers/glial markers (red) (Figures 7*B* and 8*B*).

In normal adult mice, the number of Nestin$^+$/Ngfr$^+$ cells that differentiated into neurons was significantly higher than that of Nestin$^+$ cells ($\beta$-tubulin: 15.79% vs 12.01%, $P < .05$; HuC/D: 3.12% vs 2.22%, $P > .05$). However, there was no significant difference in proportion of differentiated into glial cells (GFAP: 10.75% vs 11.65%, $P > .05$) (Figure 8*C*). In ENS-injured mice, Nestin$^+$Ngfr$^+$ cells can differentiate into newborn neurons, and this proportion was significantly higher than that of Nestin$^+$ cells (HuC/D: 6.69% vs 3.32%, $P < .05$; $\beta$-tubulin: 22.95% vs 18.68%, $P < .05$) (Figure 8*D*). These results indicated that Nestin$^+$/Ngfr$^+$ marker is more suitable for ENPCs in vivo.

### *GDNF Secreted by BMSCs Enhanced the Proliferation, Migration, and Differentiation of ENPCs*

ENPCs were isolated and identified (Figure 9). Furthermore, the biological characteristics of ENPCs co-cultured with preconditioned BMSCs were evaluated. The proliferation ($P < .001$; Figure 10*C*) and migration ($P < .0001$; Figure 10*G*) abilities of ENPCs in the co-culture group were significantly increased. Co-culture with preconditioned BMSCs helped to reduce the apoptosis of ENPCs ($P < .05$; Figure 10*E*). Western blot analysis showed that the protein expression of neuron (PGP 9.5: $P < .01$; $\beta$-tubulin: $P < .01$) and glial cell (GFAP: $P < .01$) markers were significantly up-regulated in the co-cultured group compared with the control (Figure 10*I*).

The mechanism by which BMSCs regulate the biological characteristics of ENPCs was further explored. We demonstrated that preconditioned BMSCs expressed glial cell characteristic proteins and secreted GDNF ($P < .001$; Figure 3*B*), and then ENPCs were treated with exogenous GDNF. The results showed that GDNF significantly enhanced the proliferation ($P < .001$; Figure 10*C*) and migration ($P < .0001$; Figure 10*G*) of ENPCs, while reducing their apoptosis ($P < .05$; Figure 10*E*). Then, the GDNF gene of BMSCs was silenced with small interfering RNA (SiRNA-02), and the gene and protein expression of GDNF was down-regulated ($P < .0001$; Figure 10*A* and *B*). The results showed that the promoting effect of BMSCs on ENPCs was attenuated by BMSCs (Si-GDNF) (Figure 10*D, F, H,* and *J*). In addition, co-culture with ENPCs significantly increased the proliferation ($P < .0001$; Figure 11*A*) and decreased the apoptosis ($P < .01$; Figure 11*B*) of BMSCs compared with the control.

## Discussion

Our previous research indicated that preconditioned BMSCs promoted functional enteric nerve regeneration but not through direct transdifferentiation.[19] Exploring the source of regenerating nerves in vivo is essential for promoting ENS remodeling. In this study, we found that the regenerated neurons and glial cells originated from ENPCs in ENS-injured mice after BMSCs transplantation. Most BMSCs are located in the submucosa, and a small number of BMSCs located in the myenteric plexus can differentiate into glial cells. In vitro, preconditioned BMSCs expressed glial proteins and secreted GDNF to promote the proliferation and differentiation of ENPCs.

Recent studies have demonstrated the existence of neurogenesis in uninjured adult intestine.[28,29] Liu et al[30] found increased ENS myenteric neurons during the first 4 months after birth in mice. In addition, Kulkarni et al[20,21] proposed that ENS homeostasis was maintained by ENPCs in healthy adult mice. Our results showed that Nestin$^+$/Ngfr$^+$ cells can differentiate into neurons (HuC/D: 3.12%, $\beta$-tubulin: 15.79%) in healthy adult gut, which may be a result of external threats such as considerable mechanical, chemical, and microbial stressors.[21,31] However, study by Virtanen et al[32] did not find evidence for ENS neurogenesis in healthy adults despite using the same experimental approach as Kulkarni et al.[20] Virtanen et al examined neuronal replication but excluded neurogenesis through transdifferentiation, which may contribute to the discrepancy in results. In addition, differences in the age of mouse and the time of observation may be the reasons. We analyzed neuron proliferation in three-dimensional microscopy with 5-ethynyl-2′-deoxyuridine (EdU)-labeled longitudinal muscle-myenteric plexus (LM-MPs) from the colon, HuC/D (green) and EdU (red). Some EdU-labeled LM-MPs revealed a positive overlap in two-dimensional microscopy; three-dimensional analysis revealed overlap of HuC/D/EdU labeling (Figure 12*A*). However, some EdU-labeled LM-MPs revealed a false positive in two-dimensional microscopy; three-dimensional analysis revealed that cells were layered on top of each other along the z-axis (Figure 12*B*). This would lead to overestimate the number of regenerated neurons. Three-dimensional microscopy was requested in the future.

To determine whether ENPCs are the source of regenerated neurons in mice with ENS injury, we used a triple-transgenic mouse strain (Nestin-creert2 × Ngfr-Dreert2: DTRGFP mice). Unfortunately, mice died immediately after diphtheria toxin (DT) induction, proving that Nestin$^+$/Ngfr$^+$ cells were necessary for survival. In the BAC group, we extended the area of the denervated segment and marked

with 7/0 nylon to eliminate the influence of peripheral myenteric neurons.[33] We found that 0.05% BAC led to sufficient and highly reproducible denervation of the target area for at least 31 days. In the BMSCs transplantation group, a few transplanted BMSCs located in myenteric plexus differentiated into glial cells. Nearly 22.95% of Nestin$^{+}$/Ngfr$^{+}$ cells differentiated into newborn neurons (β-tubulin), and nearly15.78% of Nestin$^{+}$/Ngfr$^{+}$ cells differentiated into newborn glial (GFAP) at day 28. These results indicated that ENPCs maintained neuronal homeostasis in mice with ENS injury. In addition, the proportion of Nestin$^{+}$/Ngfr$^{+}$ cells differentiated into neurons was significantly higher than that of Nestin$^{+}$ cells, indicating that the Nestin$^{+}$/Ngfr$^{+}$ marker was more suitable for ENPCs.

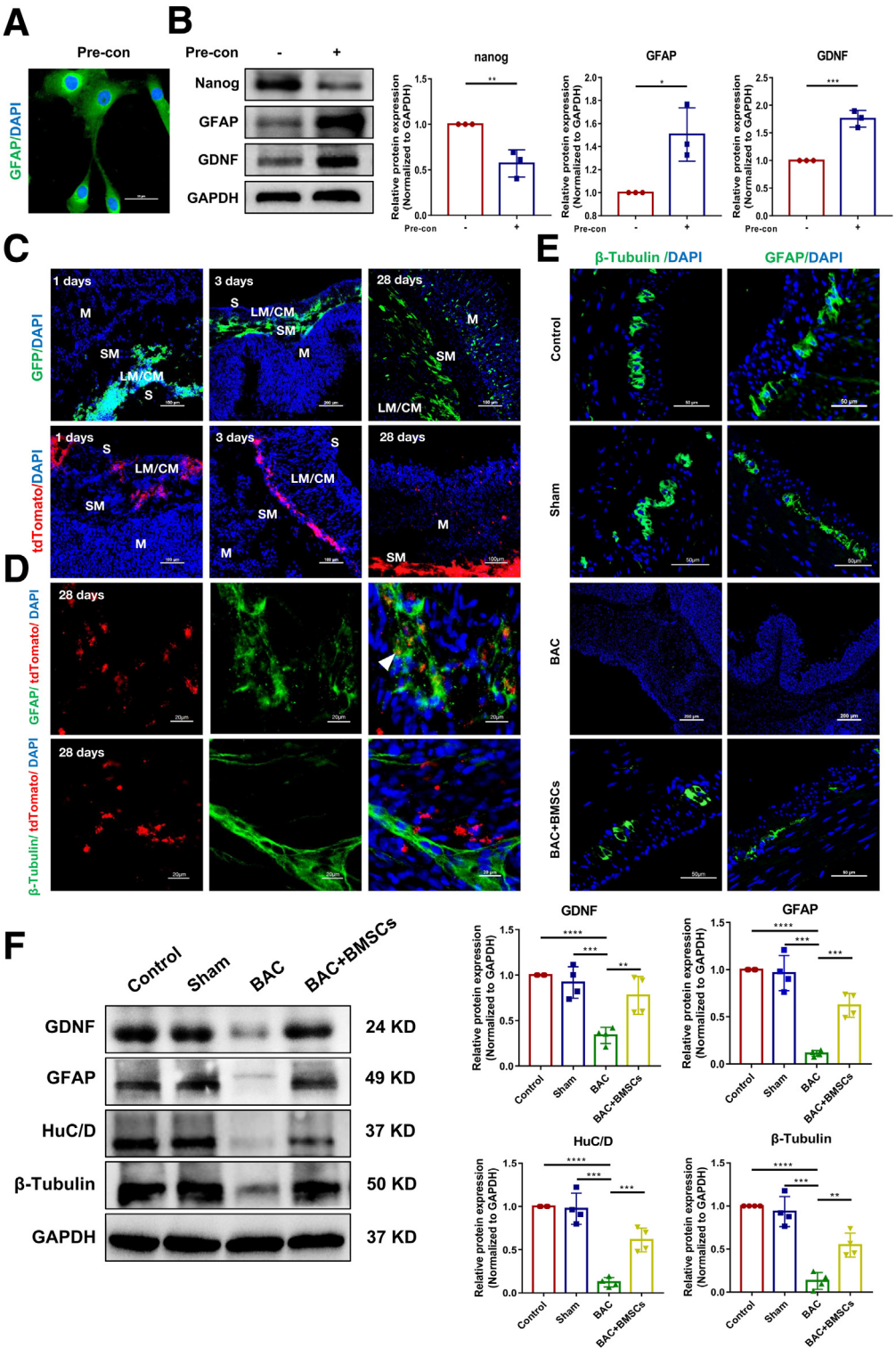

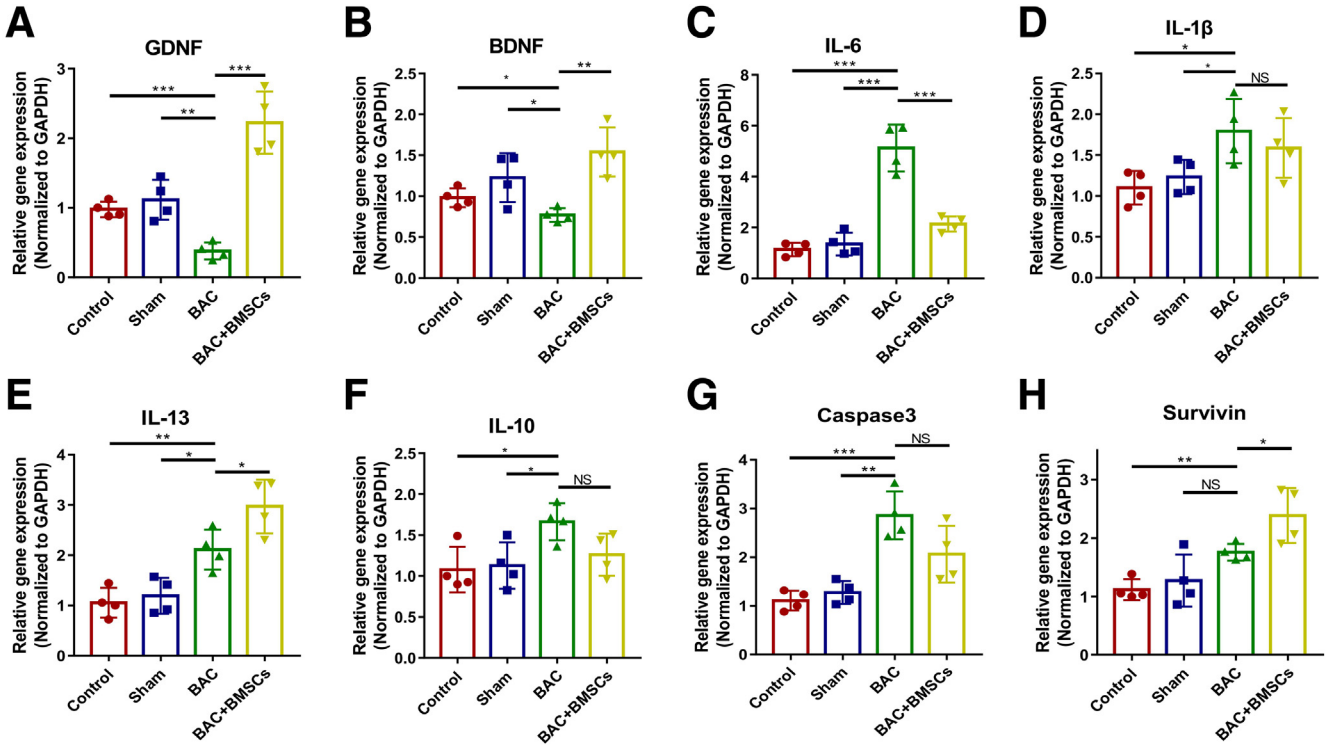


**Figure 4. Expression levels of neurotrophic factor genes (GDNF/BDNF), inflammatory cytokines (IL-6/IL-1$\beta$), anti-inflammatory factor (IL-10/IL-13), and apoptosis-related genes (Caspase 3, Survivin) for gastric tissue in different groups of mice.** *(A* and *B)* Neurotrophic factor genes (GDNF/BDNF) were decreased in ENS injury mice compared with control/sham, and BMSCs transplantation up-regulates the level of GDNF/BDNF. *(C–F)* Inflammatory cytokines (IL-1$\beta$/IL-6) and anti-inflammatory (IL-13/IL-10) were increased in BAC mice compared with control/sham, and BMSCs transplantation reduced the level of inflammatory cytokines (IL-6) and increased the level of anti-inflammatory (IL-13). *(G* and *H)* The apoptosis related genes (Caspase 3) and anti-apoptosis related genes (Survivin) were increased in ENS injury mice compared with control, and BMSCs transplantation increased the level of anti-apoptosis related genes (Survivin). Control, the control C57 mice; Sham, sham operation group; BAC, benzalkonium chloride treated group; BAC+BMSCs, BAC treated mice transplanted with BMSCs; EFS, electrical field stimulation. Results were expressed as mean ± standard deviation. $^{*}P < .05$, $^{**}P < .01$, $^{***}P < .001$, NS, no significance.

Laranjeira et al[34] reported that mouse neural crest cells marked by SRY box–containing gene 10 (SOX10) can undergo neurogenesis in response to injury. These results suggested that there may be more than one source of regenerated nerves after nerve injury.

Accumulating evidence has revealed that mesenchymal stem cells can mediate neuroprotection and repair via support, immunomodulatory, and anti-apoptosis effects.[35–37] Consistent with previous studies, our results showed that preconditioned BMSCs could express glial cell markers in vitro.[38,39] In addition, the preconditioned BMSCs can survive and express glial cell characteristic proteins in ENS-injured mice. Glial cells can secrete neurotrophic factors to alleviate neurologic defects and promote functional recovery[40,41] by promoting their development and survival and preventing neuronal apoptosis.[42,43] GDNF is an important

**Figure 3. (See previous page). BMSCs expressing glial cell characteristic protein promoted gastrointestinal nerve regeneration in denervated mice.** *(A)* BMSCs expressed glial markers (GFAP) after pre-induction. *(B)* Representative immunoblot bands and histogram of relative expression of nanog/GFAP/GDNF (normalized to GAPDH) in BMSCs after preconditioned for 10 days. *(C)* Distribution of GFP (*green*)/tdTomato (*red*)-labeled BMSCs in mouse stomach was observed by laser confocal immunofluorescence 1/3/28 days after transplantation. *(D)* Representative immunofluorescence images in gastric myenteric plexus of GFAP/$\beta$-tubulin (*green*) and tdTomato-labeled BMSCs (*red*) at 28 days after transplantation. $GFAP^{+}$ (*green*) cells in the myenteric ganglia emerge that express tdTomato (*red*) and fluoresce *yellow* (marked here by *white arrow*). *(E)* Representative immunofluorescence confocal laser images in transverse sections of gastric tissue sections of GFAP/$\beta$-tubulin (*green*) in each group (Control/Sham/BAC/BAC+BMSCs), the nuclei (*blue*). *(F)* Representative immunoblot bands and histogram of relative expression for GDNF/GFAP/HuC/D/$\beta$-tubulin in the gastric tissues (normalized to GAPDH). S, subserosa; LM, longitudinal muscle; CM, circular muscularis; SM, submucosa; M, mucosal layer; Control, the control C57 mice; Sham, sham operation group; BAC, benzalkonium chloride treated group; BAC+BMSCs, BAC treated mice transplanted with BMSCs. These results are representative of at least 3 times independent experiments. Results were expressed as mean ± standard deviation. $^{**}P < .01$, $^{***}P < .001$, $^{****}P < .0001$.

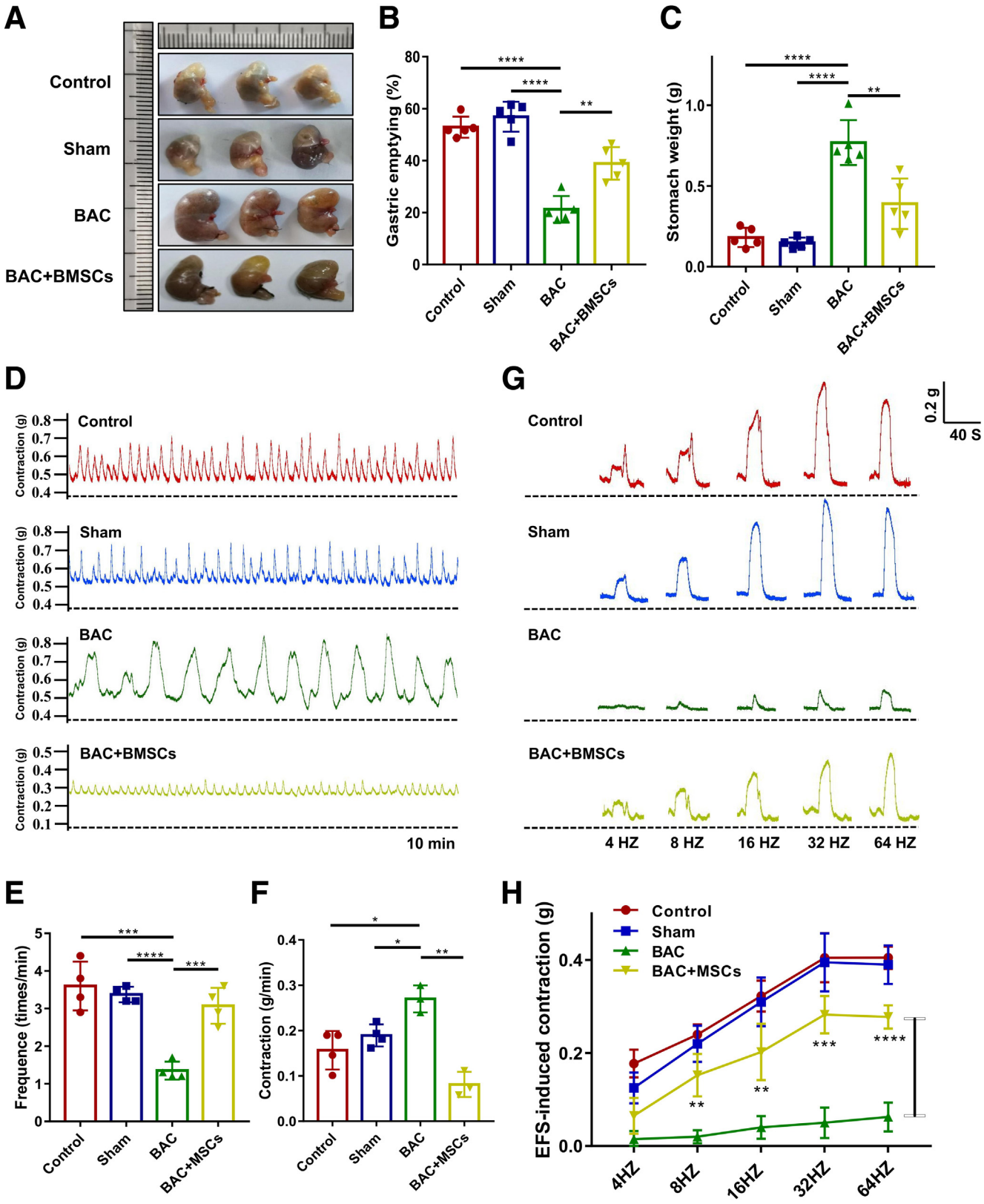


**Figure 5. BMSCs promoted recovery of gastrointestinal motility in BAC+BMSCs mice.** *(A–C)* The visual observation and gastric emptying and stomach weight were recorded after the administration of test meal. *(D)* Representative basal curves of isometric tension of circular gastric muscle strips. *(E)* Frequency of gastric muscles strip contraction in each group (10 minutes). *(F)* Contractility of gastric muscle strips in each group (analyzed as grams for 1 minute). *(G)* Representative schematic diagram of gastric muscle strips contraction response induced by EFS at increasing frequency of stimulation in each group (4–64 Hz). *(H)* Quantification of gastric strip contraction in response to EFS in each group. Control, the control C57 mice; Sham, sham operation group; BAC, benzalkonium chloride treated group; BAC+BMSCs, BAC treated mice transplanted with BMSCs; EFS, electrical field stimulation. Results were expressed as mean ± standard deviation. *$P < .05$, **$P < .01$, ***$P < .001$, ****$P < .0001$, n = 4–5.

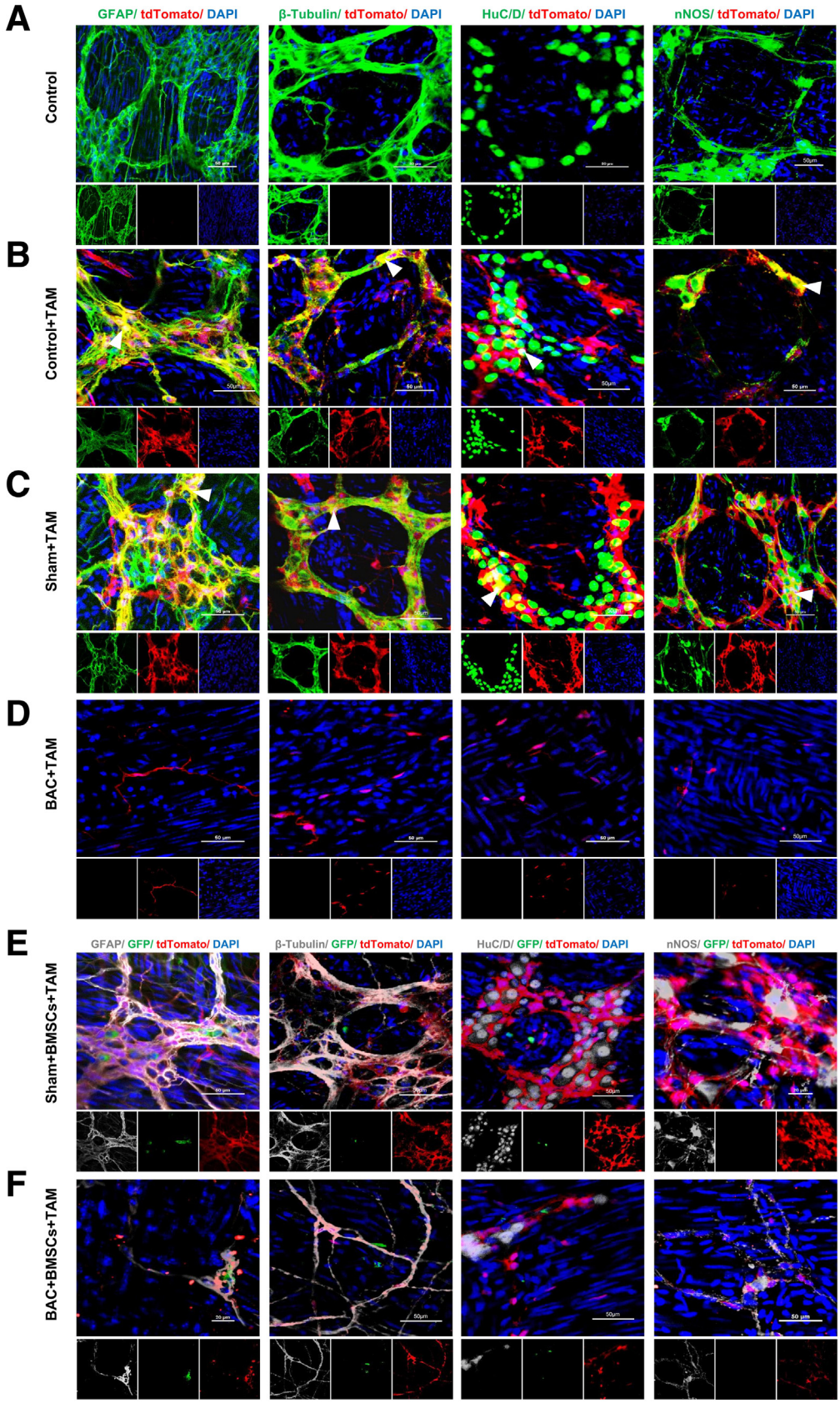


**Figure 6. Regenerated neurons derived from Nestin$^+$ cells in denervated double-transgenic mice (Nestin-creERT2: tdTomato).** *(A–D)* Representative immunofluorescence confocal laser images in freshly intermuscular plexus tissues of gastric of GFAP/$\beta$-tubulin/ HuC/D/nNOS (*green*) and tdTomato-labeled Nestin$^+$ cells (*red*) in Control, Control+TAM, Sham+TAM, and BAC+TAM groups, the nuclei (*blue*). *Arrows* indicate double-positive cells. Nestin$^+$ cells are stained with td-Tomato (*red*) and express GFAP/$\beta$-tubulin/ HuC/D/nNOS (*green*) after TAM induction and show co-localization, providing evidence that Nestin$^+$ cells can be differentiated into neurons and glial. *(E* and *F)* Representative immunofluorescence confocal laser images in freshly intermuscular plexus tissues of gastric of GFAP/$\beta$-tubulin/ HuC/D/nNOS (*gray*), tdTomato-labeled Nestin$^+$ cells (*red*), and GFP-labeled BMSCs (*green*) in Sham+BMSCs+TAM and BAC+BMSCs+TAM grou ps, the nuclei (*blue*). Control, the control C57 mice; Sham, sham operation group; BAC, benzalkonium chloride treated group; BAC+BMSCs, BAC trea ted mice transplanted with BMSCs; TAM, tamoxifen.

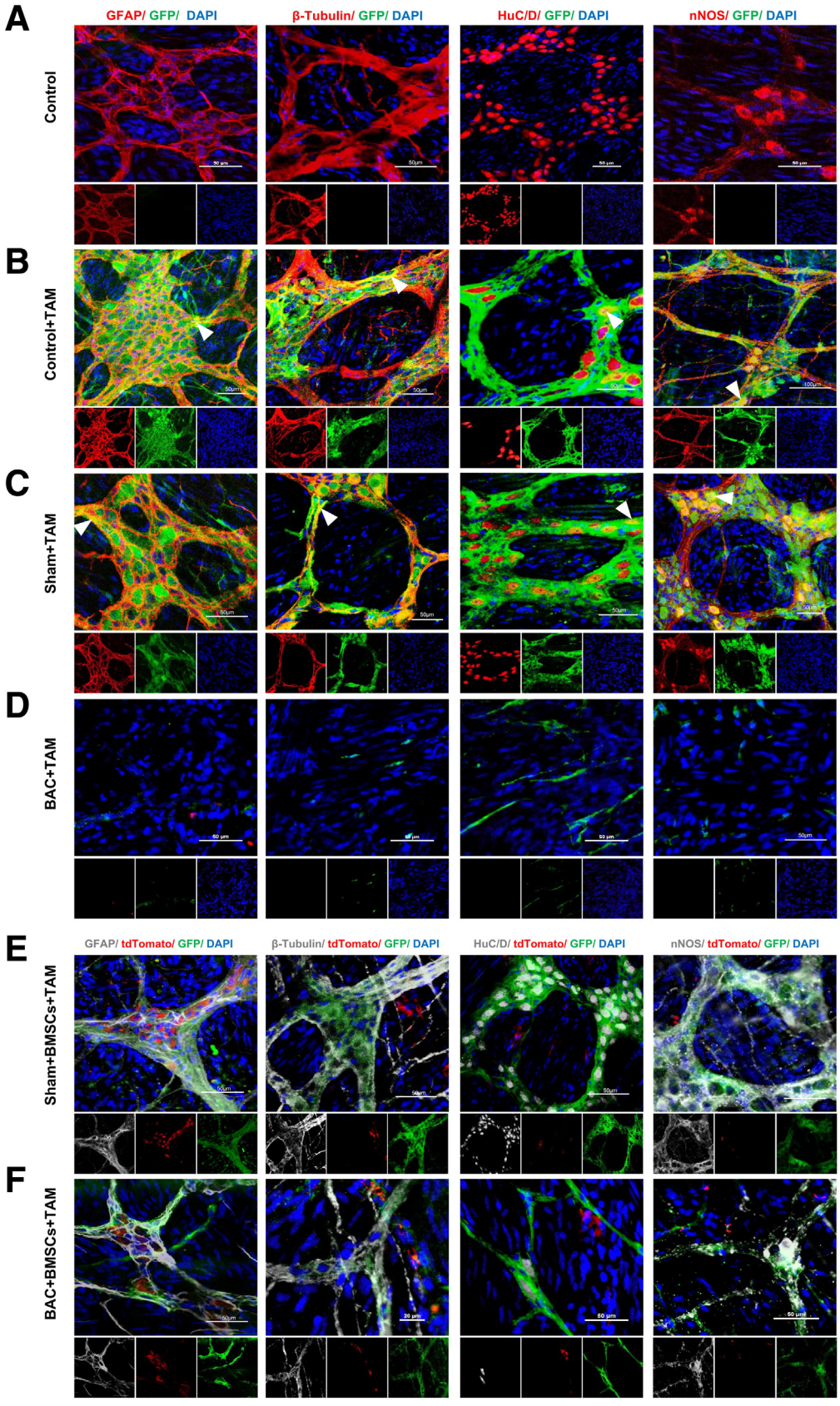


**Figure 7. Regenerated neurons derived from Nestin$^{+}$/Ngfr$^{+}$ cells in denervated triple-transgenic mice (Nestin-creERT2 × Ngfr-DreERT2: DTRGFP).** *(A–D)* Representative immunofluorescence confocal laser images in freshly intermuscular plexus tissues of gastric of GFAP/β-tubulin/HuC/D/nNOS (*red*) and GFP-labeled ENPCs (*green*) in Control, Control+TAM, Sham+TAM, and BAC+TAM, the nuclei (*blue*). *Arrows* indicate double-positive cells. Nestin$^{+}$/Ngfr$^{+}$ cells are stained with GFP (*green*) and express GFAP/β-tubulin/ HuC/D/nNOS (*red*) after TAM induction and show co-localization providing evidence that Nestin$^{+}$/Ngfr$^{+}$ cells can be differentiated into neurons and glial. *(E* and *F)* Representative immunofluorescence confocal laser images in freshly intermuscular plexus tissues of gastric of GFAP/β-tubulin/ HuC/D/nNOS (*gray*), GFP-labeled ENPCs (*green*), and tdTomato-labeled BM SCs (*red*) in Sham+BM SCs+TAM and BAC+BM SCs+TAM groups, the nuclei (*blue*). Control, the control C57 mice; Sham, sham operation group; BAC, benzalkonium chloride treated group; BAC+BMSCs, BAC treated mice transplanted with BMSCs; TAM, tamoxifen.

glial cell neurotrophic factor for the development of ENS.[27,44] McKeown et al[44] reported that the ability of enteric neural progenitors to generate ENS was enhanced when exposed to GDNF. Compared with the controls, enteric neurosphere cells exposed to GDNF showed a 14-fold increase in volume, 12-fold increase in cell number, and 2-fold increase in distance migrated. Previous studies have shown that GDNF treatment using rectal enemas induces enteric neurogenesis and

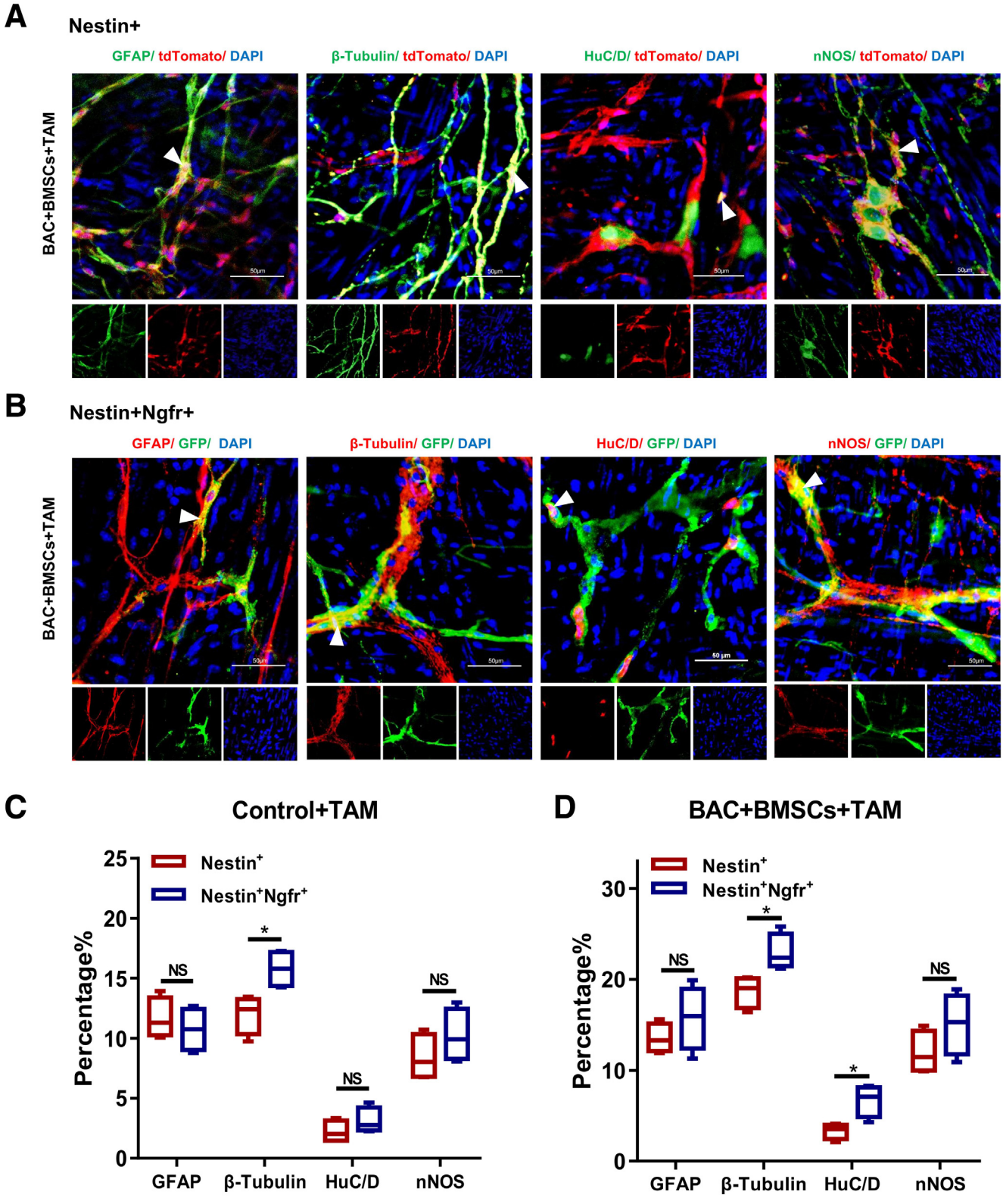

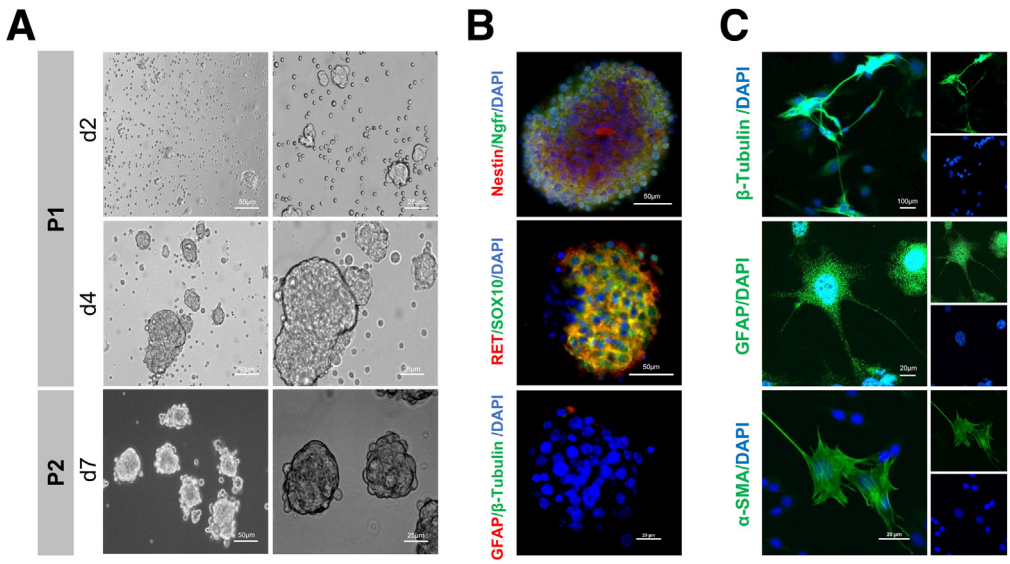


**Figure 9. Representative photographs of ENPC culture and differentiation.** *(A)* Cell morphology of ENPCs at 2, 4, and 7 days in culture. *(B)* ENPCs contain numerous cells immunopositive for Ngfr (*green*) and Nestin (*red*); ENPCs contain numerous cells immunopositive for SOX10 (*green*) and RET (*red*); ENPCs contain few cells immunonegative for $\beta$-tubulin (*green*) or GFAP (*red*). *(C)* Immunofluorescence staining indicated that ENPCs expressed neurons (PGP 9.5, $\beta$-tubulin), glial (GFAP), and smooth muscle cells ($\alpha$-SMA) marker.

improved colon structure and function in mouse models of Hirschsprung disease.[27] However, administered GDNF primarily acts during the treatment period, and multiple repetitions are required. In our study, stable high level of GDNF expression was detected after BMSCs transplantation. In addition, GDNF secreted by BMSCs enhanced the proliferation, migration, and differentiation of ENPCs in vivo.

Restoration of gastrointestinal motility is the key to cellular therapies. Our study showed that gastric motility including gastric emptying capacity and gastric muscle strip contractility were significantly increased after BMSCs transplantation. The nNOS neurons are involved in the regulation of gut motility,[45] and defects in nNOS neurons may lead to gastrointestinal motor dysfunction.[46] Our results clearly indicate that BMSCs transplantation can promote the regeneration of nNOS neurons. However, the regeneration of neural network and the recovery of gastrointestinal motility in ENS-injured mice with BMSCs transplantation are still far from normal. Therefore, exploring the optimal conditions for BMSCs transplantation is of great significance for realizing ENS remodeling. Although accurate cell targeting injections can induce a large number of cells during surgery, this invasive procedure may result in tissue damage.[47] The clinical application of endoscopic ultrasound should be considered in the future to allow accurate targeting of specific layers of the gut and reduce tissue damage.

In summary, our study provides the first evidence that GDNF secreted by BMSCs promotes the proliferation and differentiation of ENPCs in vitro. In vivo, BMSCs function as glial cells to promote the differentiation of ENPCs into neurons and glial cells. Our study provides a scientific foundation for the treatment of ENS-related disorders and further promotes the clinical application of BMSCs-based therapies in the future.

## Materials and Methods

### Animals

Nestin-creert2 mice were bred with Rosa26-LSL-tdTomato mice to generate double-transgenic mice: Nestin-creert2: tdTomato mice. After TAM induction, Nestin$^+$ cells were labeled with tdTomato (Figure 13*A*). In addition, only homozygous mice were used to trace the

**Figure 8.** (***See previous page***). **Proportion of Nestin$^+$/Ngfr$^+$ cells differentiated into neurons was significantly higher than that of Nestin$^+$ cells.** *(A)* Representative immunofluorescence confocal laser images in freshly intermuscular plexus tissues of gastric of GFAP/$\beta$-tubulin/HuC/D/nNOS (*green*) and tdTomato-labeled Nestin$^+$ cells (*red*) in BAC+BMSCs+TAM (Nestin-creERT2: tdTomato mice), the nuclei (*blue*). *Arrows* indicate double-positive cells. *(B)* Representative immunofluorescence confocal laser images in freshly intermuscular plexus tissues of gastric of GFAP/$\beta$-tubulin/HuC/D/nNOS (*red*) and GFP-labeled Nestin$^+$/Ngfr$^+$ cells (*green*) in BAC+BMSCs+TAM (Nestin-creert2 X Ngfr-Dreert2: DTRGFP mice), the nuclei (*blue*). *Arrows* indicate double-positive cells. *(C* and *D)* Proportion of Nestin$^+$ (*red*)/Nestin$^+$Ngfr$^+$ (*blue*) cells differentiated into neurons and glial cells in Control+TAM group and BAC+BMSCs+TAM group. Control, the control C57 mice; Sham, sham operation group; BAC, benzalkonium chloride treated group; TAM, tamoxifen. These results are representative of independent experiments repeated at least 3 times. Results were expressed as mean ± standard deviation. $^*P < .05$, $^{**}P < 0.01$, NS, no significance.

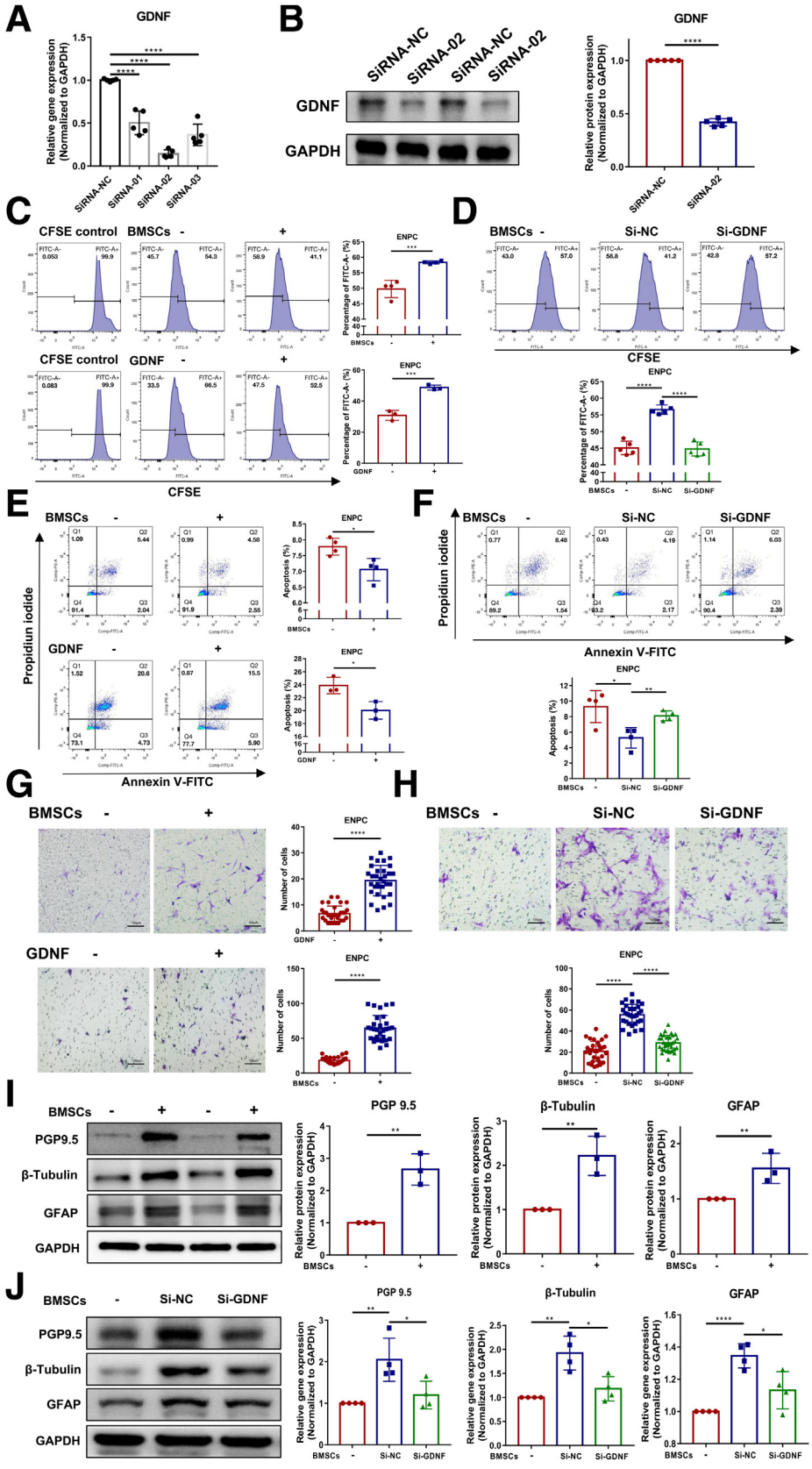


**Figure 10. Preconditioned BMSCs promote proliferation, migration, and differentiation of ENPCs by secreting GDNF.** *(A)* RT-qPCR confirmation of successful GDNF gene knockdown after GDNF-specific SiRNA transfection compared with SiRNA-NC transfection. *(B)* Representative immunoblot bands and histogram of relative expression of GDNF protein in BMSCs (SiRNA-NC) and BMSCs (SiRNA-02). *(C)* Representative CFSE-labeled ENPCs and percentage of cells in FITC-A- after co-culture with BMSCs/GDNF for 48 hours. *(D)* Representative CFSE-labeled ENPCs and percentage of cells in FITC-A- after co-culture with BMSCs (-, Si-NC, Si-GDNF) for 48 hours. *(E)* Apoptosis rate (percentage of cells in Q2/Q3) of ENPCs after co-culture with BMSCs/GDNF for 48 hours was detected by flow cytometry assay. *(F)* Apoptosis rate (percentage of cells in Q2/Q3) of ENPCs after co-culture with BMSCs (-, Si-NC, Si-GDNF) for 48 hours was detected by flow cytometry assay. *(G)* Transwell migration assay of ENPCs after co-culture with BMSCs/GDNF for 48 hours. *(H)* Transwell migration assay of ENPCs after co-culture with BMSCs (-, Si-NC, Si-GDNF) for 48 hours. *(I* and *J)* Representative immunoblot bands and histogram of relative expression of PGP9.5/$\beta$-tubulin/GFAP in ENPCs after co-culture with BMSCs (-, Si-NC, Si-GDNF) in vitro for 48 hours. RT-PCR, reverse transcriptase polymerase chain reaction; SiRNA-NC, BMSCs transfected with SiRNA negative control; SiRNA-01, BMSCs transfected with SiRNA-GDNF-01; SiRNA-02, BMSCs transfected with SiRNA-GDNF-02; SiRNA-03, BMSCs transfected with SiRNA-GDNF-03; Si-GDNF, BMSCs transfected with SiRNA-GDNF; GDNF, glial cell-derived neurotrophic factor; CFSE, 5-(and 6)-carboxyfluorescein diacetate succinimidyl ester. These results are representative of at least 3 times independent experiments. Results were expressed as mean ± standard deviation. $^{*}P < .05$, $^{**}P < .01$, $^{***}P < .001$, $^{****}P < .0001$.

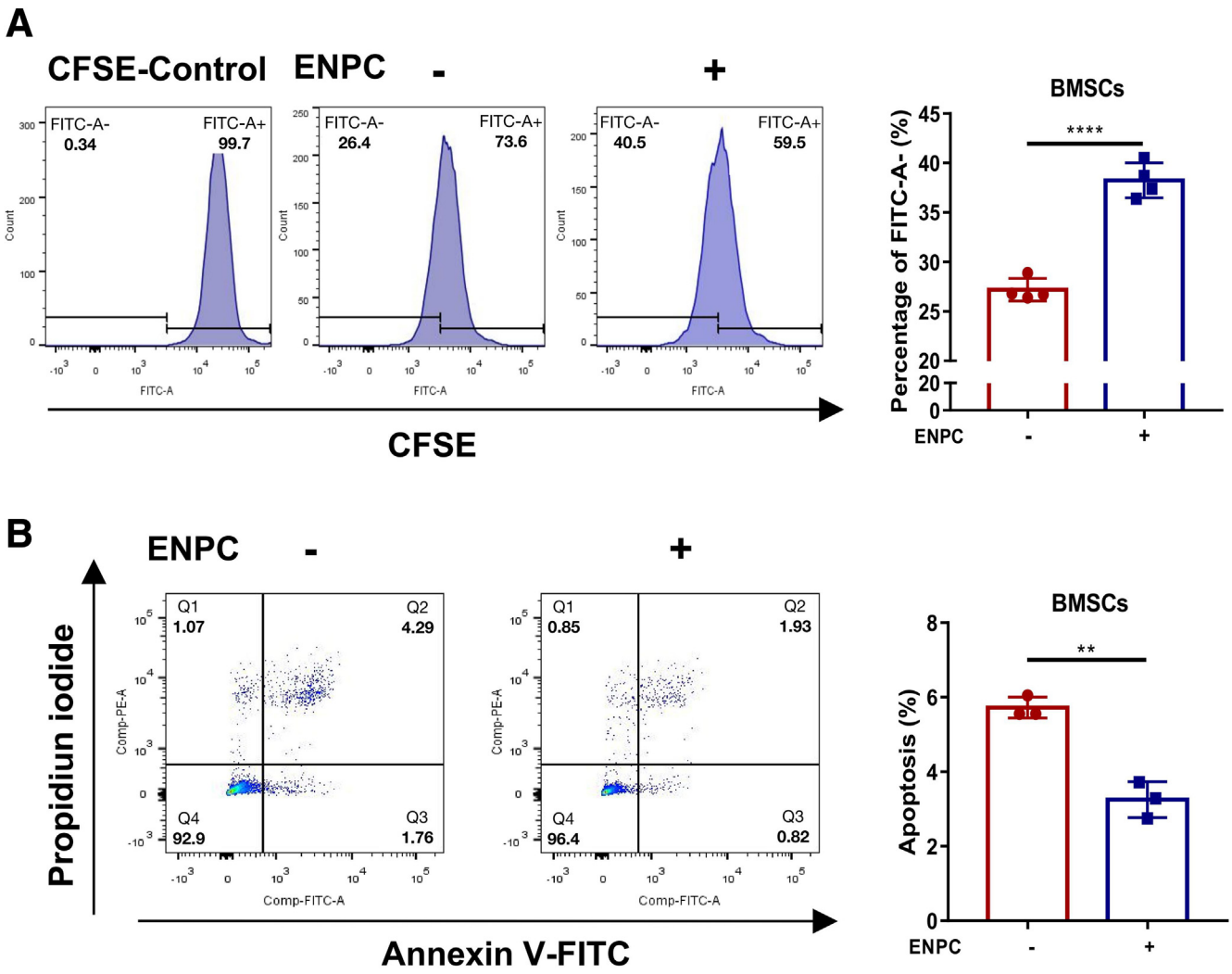


**Figure 11. ENPCs promote proliferation and decrease apoptosis of BMSCs in vitro.** *(A)* Representative CFSE-labeled BMSCs and percentage of BMSCs in FITC-A- after co-culture with ENPCs in vitro for 48 hours. *(B)* Apoptosis rate (percentage of cells in Q2/Q3) of BMSCs after co-culture with ENPCs for 48 hours was detected by flow cytometry assay. CFSE, 5-(and 6)-carboxyfluorescein diacetate succinimidyl ester. These results are representative of at least 3 times independent experiments. Results were expressed as mean ± standard deviation. $^{**}P < .01$, $^{****}P < .0001$.

fate of Nestin$^+$ cells in vivo. In addition, Nestin-creert2 mice were bred with R26-e(CAG-RSR-LSL-DTRGFP-WPRE-pA) × Ngfr-e(2A-DreERT2) mice to generate triple-transgenic mice: Nestin-creert2 × Ngfr-Dreert2: DTRGFP. After TAM induction, Nestin$^+$/Ngfr$^+$ cells were labeled with GFP to track Nestin$^+$/Ngfr$^+$ cells (Figure 13*C*). Moreover, Nestin$^+$/Ngfr$^+$ cells were knocked out after DT induction. Nestin-creert2, Rosa26-LSL-tdTomato, Ngfr-e(2A-DreERT2), R26-e(CAG-RSR-LSL-DTRGFP-WPRE-pA), and tdTomato mice were purchased from Shanghai Model Organisms Center, Inc (Shanghai, China). Wild-type C57BL/6J and GFP mice were purchased from Beijing HFK Biotechnology Co, Ltd (Beijing, China). Pregnant female mice (C57BL/6J, embryonic period 16-18 days [E16-18]) were used to isolate ENPCs. All the mice were housed in a specific pathogen-free facility under controlled temperature and photoperiod conditions. All animal studies were approved by the Animal Care and Use Committee of Union Hospital at Tongji Medical College, Huazhong University of Science and Technology (S2804).

## Tamoxifen Induction

Tamoxifen (Sigma-Aldrich, St Louis, MO; cat. #10540-29-1) was dissolved in corn oil at a concentration of 20 mg/mL and stored at 4°C.[20] To label Nestin$^+$ cells with tdTomato in Nestin-creERT2: tdTomato mice for fate mapping experiments in vivo, 3 doses of TAM (100 $\mu$L) were intraperitoneally administered on 3 consecutive days. To label Nestin$^+$/Ngfr$^+$ cells with GFP in Nestin-creert2 × Ngfr-Dreert2: DTRGFP mice for fate mapping experiments

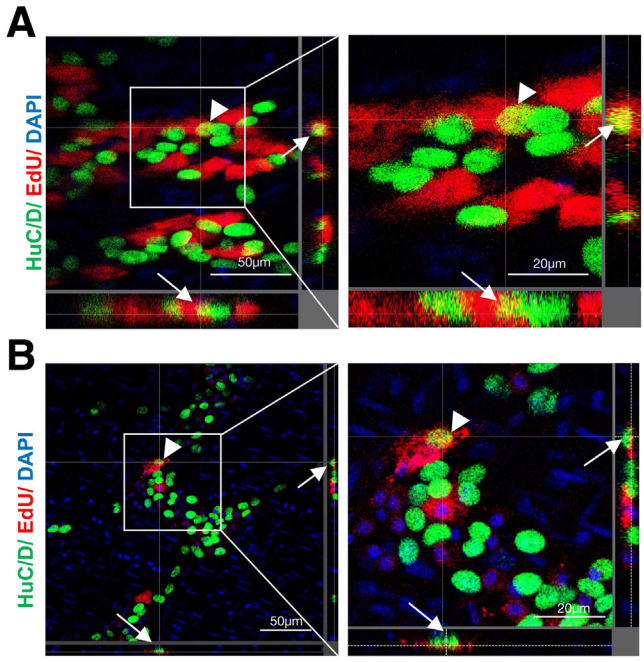


**Figure 12. Analysis of neuron proliferation in the colon in three-dimensional (3D) microscopy.** Analysis of EdU-labeled LM-MPs from the colon, HuC/D (*green*) and EdU (*red*). *(A)* EdU-labeled LM-MPs revealed double-positive HuC/D/EdU enteric neurons. 3D analysis revealed overlap of HuC/D/EdU labeling, appearing as true positives in 2D microscopy. *(B)* EdU-labeled LM-MPs revealed putative overlap of HuC/D/EdU labeling. 3D analysis revealed that cells were layered on top of each other along the z-axis, appearing as false positives in 2D microscopy. EdU, 5-ethynyl-2′-deoxyuridine; LM-MPs, longitudinal muscle-myenteric plexus.

in vivo, 6 doses of TAM (100 $\mu$L) were intraperitoneally administered on 6 consecutive days.

## Diphtheria Toxin Induction

DT (Merck-Millipore, Burlington, MA; cat. #322326) was dissolved in phosphate-buffered saline (PBS) at a concentration of 2 $\mu$g/$\mu$L and stored at −20°C. To knockout Nestin$^{+}$/Ngfr$^{+}$ cells in Nestin-creert2 × Ngfr-Dreert2: DTRGFP mice, mice were intraperitoneally injected with DT (10 $\mu$g/kg/d) on days 1, 3, and 5 before surgery.

## BMSCs Isolation and Induction

BMSCs were obtained and identified as described previously.[19] GFP-labeled BMSCs were isolated from GFP mice, and tdTomato-labeled BMSCs were isolated from tdTomato mice as in our previous research (Figure 13*B* and *D*).[48] For preconduction, BMSCs at passage 6 were cultured in Dulbecco modified Eagle medium containing 10% fetal bovine serum, basic fibroblast growth factor (bFGF) (10 ng/mL; Peprotech, Rocky Hill, NJ), epidermal growth factor (EGF) (10 ng/mL; Peprotech), and GDNF (10 ng/mL; Peprotech) for 10 days. Immunofluorescence staining showed that BMSCs expressed neurons (PGP 9.5, HuC/D, $\beta$-tubulin, nNOS) and glial cell (GFAP positive) markers after being preconditioned for 10 days (Figure 14).

## Grouping and BMSCs Transplantation

Wild-type C57BL/6J mice (8–10 weeks) were randomly divided into 4 groups: control, sham, BAC treatment, and BAC + BMSCs. In the sham group, the animals were anesthetized by intraperitoneal injection of sodium pentobarbital (45 mg/kg), and a midline incision was made. Second, a 1-cm segment of gastric tissue was exposed, wrapped with gauze, and soaked for 15 minutes with normal saline, and the treatment area was marked with 7/0 nylon. Third, 200 $\mu$L PBS was injected into the treated gastric subserosa using a 22-gauge needle after 3 days. In the BAC group, 0.05% BAC (Merck, Rahway, NJ; CAS:63449-41-2) was administered instead of normal saline, and the other treatments were administered as described for the sham group. In the BAC + BMSCs group, BMSCs ($2 \times 10^6$ cells in 0.2 mL PBS) were transplanted into the denervated gastric subserosa with a 22-gauge needle at 4 sites 3 days after BAC treatment, and the other treatments were administered as described in the BAC group. In addition, the transgenic mice (8–10 weeks) were divided into 6 groups: control, control + TAM, sham + TAM, BAC + TAM, sham + BMSCs + TAM, and BAC + BMSCs + TAM. TAM was administered intraperitoneally after BMSCs/PBS injection. DT induction was conducted to knockout Nestin+/Ngfr+ cells in Nestin-creert2 × Ngfr-Dreert2: DTRGFP mice. Four weeks after BMSCs transplantation, the mice were euthanized, and their tissues were collected for subsequent analysis.

## ENPC Isolation and Culture

ENPCs were harvested from E16 mice. Whole guts of E16 embryos were dissected, washed with $Ca^{2+}$/$Mg^{2+}$-free PBS (0.1% penicillin/streptomycin), and then cut into pieces (0.5–1 mm). These pieces were enzymatically dissociated using dispase I (0.1 mg/mL), collagenase XI (300 U/mL), and dNase I (10 mg/mL) for 40 minutes at 37°C. Thereafter, the cell suspensions were filtered through a 40-$\mu$m cell strainer, centrifuged, and cultured in Dulbecco modified Eagle medium/F12 medium containing B27 (20 ng/mL, stem cell), fibroblast growth factor (FGF) (20 ng/mL; Peprotech), and EGF (20 ng/mL; Peprotech). ENPCs grew as free-floating neurospheres and were passaged every 5–7 days by incubation with Accutase (StemPro) for 15 minutes at 37°C (Figure 9*A*). Immunostaining confirmed the presence of ENPCs and revealed that they co-expressed both Nestin/Ngfr and RET proto-oncogene (RET)/SOX10 (Figure 9*B*). In addition, a few ENPCs expressed neuronal and glial cell markers (Figure 9*B*). ENPCs differentiated into neurons (PGP 9.5, $\beta$-tubulin), glial cells (GFAP), and smooth muscle cells ($\alpha$-SMA) after culturing in differentiation medium for 7 days (Figure 9*C*).

## Immunofluorescence

To investigate the morphologic changes of myenteric plexus of the stomach, the mucosa and submucosa were gently torn off with micro tweezers in pre-cooled Kreb's solution. Muscularis tissues were fixed in 4% paraformaldehyde for 12 minutes, then washed with PBS, and incubated with donkey serum containing 0.3% Triton X-100 at 4°C overnight. Then, the muscularis tissues were incubated with the primary

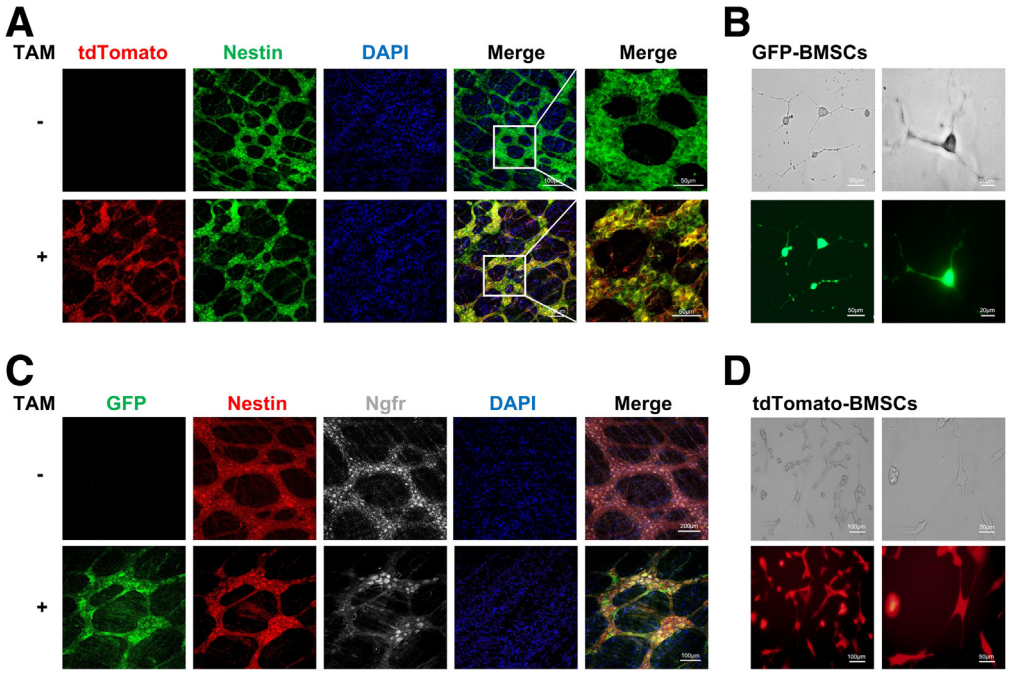


**Figure 13. Identification of Nestin-creERT2: tdTomato mice and Nestin-creERT2 X Ngfr-DreERT2: DTRGFP mice.** *(A)* Immunofluorescence staining showed the co-expression of Nestin (*green*) and tdTomato (*red*) and indicated that cells with tdTomato-positive were Nestin-positive cells, the nuclei (*blue*). *(B)* Cell morphology of GFP-labeled BMSCs after 10 days pre-conditioned. *(C)* Immunofluorescence staining showed co-expression of Nestin (*red*), Ngfr (*gray*), and GFP (*green*) and indicated that cells with GFP-positive were $Nestin^{+}Ngfr^{+}$ cells, the nuclei (*blue*). *(D)* Cell morphology of tdTomato-labeled BMSCs after 10 days pre-conditioned.

antibody (Table 1) at 4°C for 48 hours and subsequent addition of secondary antibodies (Table 1) for 2 hours. Nuclei were stained with 4′,6-diamidine-2′-phenylindole dihydrochloride (DAPI) for 10 minutes. To investigate the morphologic changes in the stomach enteric nerve in a cross section, paraffin sections of stomach tissues were deparaffinized before antigen retrieval. The cells were washed in PBS and blocked with donkey serum for 30 minutes at room temperature. The next step was the same as that described above. In addition, the slides were fixed in 4% paraformaldehyde for 20 minutes at room temperature, and the next step was the same as above. Finally, the stained sections were viewed using a confocal laser scanning microscope (BX53; Olympus, Tokyo, Japan) with the NIS Elements Viewer Software (Nikon, Tokyo, Japan).

## Western Blot Analysis

Proteins harvested from the cells and stomach muscularis tissues were homogenized in lysis buffer (radioimmunoprecipitation assay: phenylmethyl sulfonyl fluoride = 100:1). Protein concentration was evaluated using the bicinchoninic acid method. Equal amounts of protein were subjected to 12.5% sodium dodecyl sulfate-polyacrylamide gel electrophoresis and transferred to polyvinylidene fluoride membranes. After soaking in 10% nonfat dry milk at room temperature for 1 hour, membranes were incubated with specific primary antibodies (Table 1) at 4°C overnight. Then the membranes were incubated with specific secondary antibodies (AntGene, Wuhan, China) for 1 hour at 37°C. Finally, the bands were visualized by chemiluminescence immunoassay using an enhanced chemiluminescent agent (Thermo Fisher Scientific Inc, Waltham, MA). The intensities of the bands were quantified using ImageJ v1.51.

## Gastric Emptying

The mice were fasted overnight. Twenty minutes before euthanizing, 300 $\mu$L of test meal (containing phenol red and carboxymethylcellulose) was administered to mice by gavage. The stomach contents were placed in 10 mL NaOH (0.1N). Phenol red content was measured according to the method as previously described.[49] Gastric emptying (%) = $100 \times (1 - X/Y)$ (X, absorbance of test mice; Y, absorbance of control mice immediately collected by gavage).

## Smooth Muscle Activity Recording

Gastric muscle strips were suspended between two L-shaped hooks in a 25 mL organ bath with oxygenated Kreb's solution (composed of 118.3 mmol/L NaCl, 4.7 mmol/L KCl, 1.2 mmol/L $MgSO_4$, 1.2 mmol/L $K_2HPO_4$, 2.5 mmol/L $CaCl_2$, 25 mmol/L $NaHCO_3$, and 11.1 mmol/L D-glucose) at 37°C (95% $O_2$, 5% $CO_2$). The muscle strips were equilibrated for 1 hour under a preload of 1 g, and a stable spontaneous contractile pattern was obtained. EFS, which elicited neural activation-mediated muscle contraction, was conducted (20 V, 10 seconds). Contractile activity was measured using an isometric force transducer (ADInstruments, Dunedin, New Zealand). The contractile curve was consecutively recorded and analyzed using the LabChart software (version 7.0; ADInstruments).

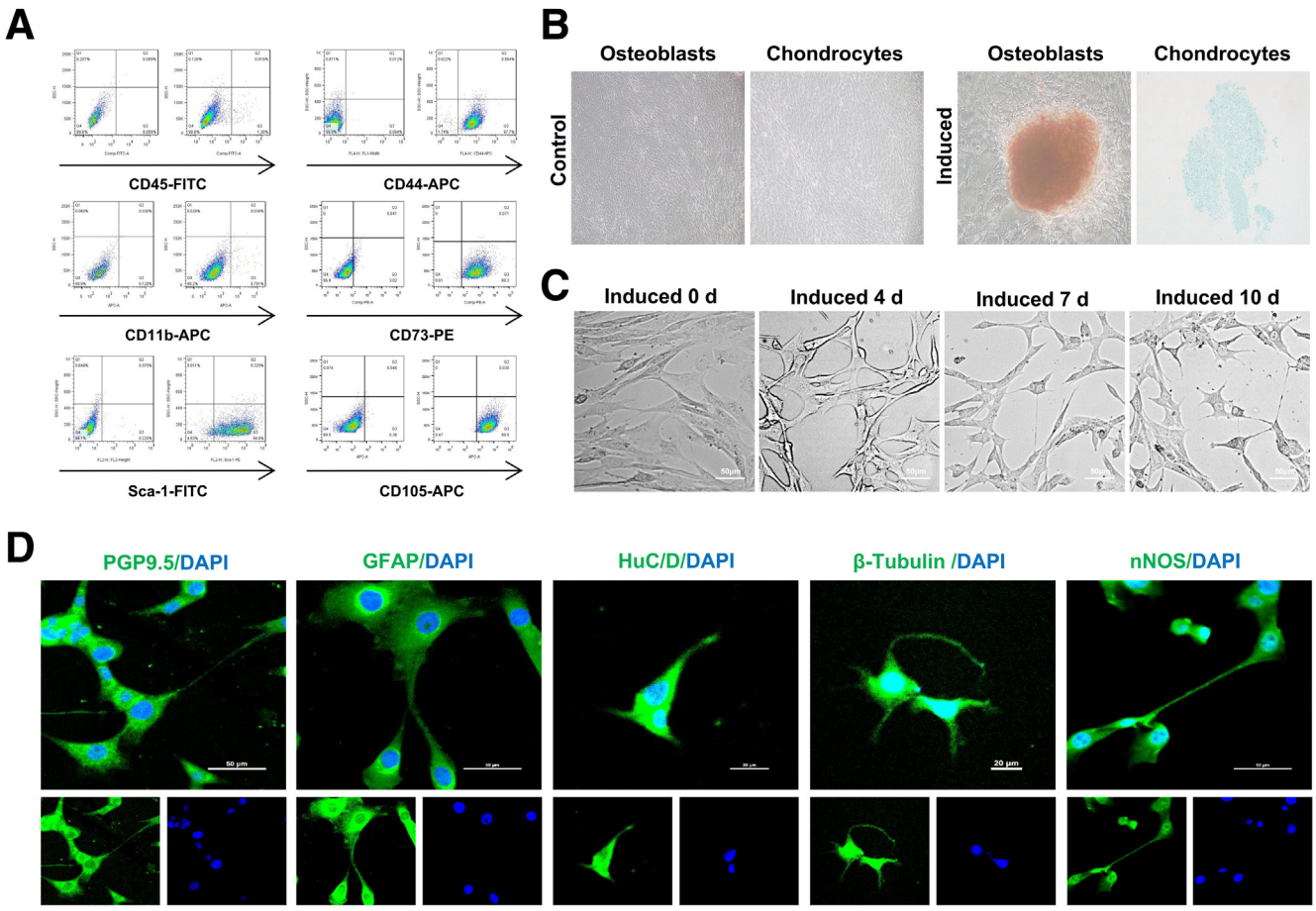


**Figure 14. Representative photographs of BMSCs identification and pre-conditioned.** *(A)* Flow cytometric analysis of CD45, CD44, CD11b, CD-73, Sca-1, and CD105, respectively. *(B)* BMSCs were cultured in osteogenic medium and chondrogenic medium and stained with Alizarin red and Alcian blue to identify differentiation. *(C)* Cell morphology of BMSCs pre-conditioned at 0, 4, 7, and 10 days. *(D)* Immunofluorescence staining showed that BMSCs expressed neurons (PGP 9.5, HuC/D, $\beta$-tubulin, nNOS) and glial cell (GFAP positive) marker after pre-conditioned for 10 days.

## SiRNA Transfection

The SiRNA oligo used for GDNF gene silencing was purchased from Wuhan Qingke Co, Ltd (Wuhan, China). SiRNA-01 (sense: 5′-CGGUAAGAGGCUUCUCGAATT-3′, antisense: 5′-UUCGAGAAGCCUCUUACCGTT-3′); SiRNA-02 (sense: 5′-CGGAGUAGAAGGCUAACAATT-3′, antisense: 5′-UUGUUAGCCUUCUACUCCGTT-3′); SiRNA-03 (sense: 5′-CCAAUAUGCCUGAAGAUUATT-3′, antisense: 5′-UAAUCUUCAGGCAUAUUGGTT-3′). GDNF SiRNA was transfected into BMSCs at a concentration of 100 nmol/L using Lipofectamine 3000 reagent (Invitrogen, Waltham, MA) according to the manufacturer's instructions. The supernatant was discarded 6 hours after transfection and replaced with a fresh medium. Further analysis was performed 48 hours after transfection.

## Quantitative Reverse Transcriptase Polymerase Chain Reaction

RNA was isolated using TRIzol reagent (Vazyme, China) in accordance with the manufacturer's protocol, and cDNA was generated using a cDNA synthesis kit (Takara Bio, Shiga, Japan). Quantitative polymerase chain reaction analyses were performed using the StepOne Real-Time PCR system (Applied Biosystems, Waltham, MA). Threshold cycle (Ct) values were normalized against GAPDH using the ΔΔCt method. The primer sequences used in this experiment are listed in Table 2.

## Proliferation

Cells were resuspended in PBS at 5–10 $\times$ $10^6$/mL and incubated with 10 $\mu$mol/L 5-(and 6)-carboxyfluorescein diacetate succinimidyl ester (Ebioscience, San Diego, CA) for 10 minutes at room temperature in the dark. The cells were then washed twice with complete medium and transferred to 6-well co-culture plates (pore size, 4 $\mu$m; Corning, Corning, NY). After co-culture for 48 hours, 5-(and 6)-carboxyfluorescein diacetate succinimidyl ester–labeled cells were collected and subjected to flow cytometry using a 488 nm excitation source.

## Apoptosis

Cell apoptosis was detected by flow cytometry analysis using annexin V/propidium (propidium iodide) staining (AntGene, Wuhan, China). After co-culture for 48 hours, the cells were harvested and washed thrice with cold PBS. The cells were then resuspended in binding buffer containing

**Table 1.** Antibodies Used and Their Concentrations

| Protein/staining target | Source | Concentration |
|---|---|---|
| Rabbit anti-PGP9.5 | Abclonal (A19101) | IF (1:200); WB (1:1000) |
| Mouse anti-$\alpha$-SMA | Boster (BM0002) | IF (1:200) |
| Rabbit anti-HuC/D | Abcam (ab184267) | IF (1:500); WB (1:1000) |
| Rabbit anti-GFAP | Abclonal (A0237) | IF (1:200); WB (1:1000) |
| Rabbit anti-$\beta$-tubulin | Abclonal (AC008) | IF (1:200); WB (1:1000) |
| Rabbit anti-nNOS | Genetex (GTX133403) | IF (1:200) |
| Goat anti-Td-tomato | Arigo (ARG55724) | IF (1:500) |
| Mouse anti-GFP | Promoter (QSJ-078) | IF (1:100) |
| Goat anti-GFP | Abcam (ab5450) | IF (1:1000) |
| Rabbit anti-Nanog | Abcam (ab80892) | WB (1:1000) |
| Rabbit anti-GDNF | Abcam (ab176564) | WB (1:1000) |
| Rabbit anti-Nestin | Abclonal (A11861) | IF (1:200) |
| Mouse anti-Ngfr | R&D Systems (AF1157) | IF (1:200) |
| Rabbit anti-SOX10 | Abcam (ab155279) | IF (1:200) |
| Goat anti-RET | R&D Systems (AF482) | IF (1:200) |
| Rabbit anti-GAPDH | Antgene, Wuhan, China | WB (1:1000) |
| Alexa Fluor 488 and donkey anti-goat IgG | AntGene, Wuhan, China | IF (1:200) |
| Alexa Fluor 488 and donkey anti-mouse IgG | AntGene, Wuhan, China | IF (1:200) |
| Alexa Fluor 488 and donkey anti-rabbit IgG | AntGene, Wuhan, China | IF (1:200) |
| Alexa Fluor 594 and donkey anti-rabbit IgG | AntGene, Wuhan, China | IF (1:200) |
| Alexa Fluor 594 and donkey anti-goat IgG | AntGene, Wuhan, China | IF (1:200) |
| Alexa Fluor 647 and donkey anti-rabbit IgG | AntGene, Wuhan, China | IF (1:200) |

IF, immunofluorescence, WB, Western blot.

**Table 2.** Primers Used for Quantitative RT-PCR

| Number | Primer for RT-PCR ( mouse ) | Forward primer | Reverse primer |
|---|---|---|---|
| 1 | GDNF | CGTCATCAAACTGGTCAGGA | CGCTGAACCACTCCCTC |
| 2 | BDNF | GCGGCAGATAAAAAGACTGC | GCAGCCTTCCTTCGTGTAAC |
| 3 | IL-6 | CTGCAAGAGACTTCCATCCAG | AGTGGTATAGACAGGTCTGTTGG |
| 4 | IL-1$\beta$ | CATCTTCTCAAAATTCGAGTGACAA | TGGGAGTAGACAAGGTACAACCC |
| 5 | IL-13 | CTTGCTTGCCTTGGTGGTCT | CACAGGGGAGTCTGGTCTTG |
| 6 | IL-10 | AAGCCTTATCGGAAATGATCCA | GCTCCACTGCCTTGCTCTTATT |
| 7 | Caspase 3 | ATGGAGAACAATAAAACCT | CTAGTGATAAAAGTAGAGTTC |
| 8 | Survivin | TTGGCAGGTGCCTGTTGAAT | AGCCAGTCCCCCACAGCAT |
| 9 | GAPDH | AGGAGCGAGACCCCACTAACA | AGGGGGGCTAAGCAGTTGGT |

RT-PCR, reverse transcriptase polymerase chain reaction.

Annexin V-FITC and PI. After incubation for 15 minutes at room temperature, the cells were analyzed using flow cytometry within 1 hour.

## Migration

Cell migration was measured using a Transwell assay (pore size, 8 $\mu$m; Corning). A total of $1 \times 10^5$ ENPCs were seeded in the upper chamber, and BMSCs or cell culture medium were seeded in the lower well for co-cultivation. After 48 hours, the cells in the upper well were stained with crystal violet and counted under a microscope.

## EdU Labeling

The LM-MPs were peeled off from colon by microdissection. LM-MPs were cultured in Dulbecco modified Eagle medium/F12 medium containing B27 (20 ng/mL; Stem cell), FGF (20 ng/mL; Peprotech), and EGF (20 ng/mL; Peprotech). EdU (Invitrogen, Carlsbad, CA) was added to media at a final concentration of 25 $\mu$mol/L for 48 hours.

Then LM-MPs were fixed, and EdU uptake was detected by immunofluorescence.

### Statistical Analysis

Data are presented as mean ± standard deviation. Statistical analyses were performed using GraphPad Prism v6.0c (San Diego, CA) and ImageJ v1.51. Student $t$ test was used to compare differences between 2 groups, and differences between multiple groups were compared using one-way analysis of variance. Statistically significant differences were defined as $^{*}P < .05$, $^{**}P < .01$, $^{***}P < .001$, and $^{****}P < .0001$.

## References


1. Rao M, Gershon MD. The bowel and beyond: the enteric nervous system in neurological disorders. Nat Rev Gastroenterol Hepatol 2016;13:517–528.
2. Furness JB. The enteric nervous system and neurogastroenterology. Nat Rev Gastroenterol Hepatol 2012;9:286–294.
3. Burns AJ, Thapar N. Neural stem cell therapies for enteric nervous system disorders. Nat Rev Gastroenterol Hepatol 2014;11:317–328.
4. Burns AJ, Goldstein AM, Newgreen DF, Stamp L, Schäfer KH, Metzger M, Hotta R, Young HM, Andrews PW, Thapar N, Belkind-Gerson J, Bondurand N, Bornstein JC, Chan WY, Cheah K, Gershon MD, Heuckeroth RO, Hofstra RM, Just L, Kapur RP, King SK, McCann CJ, Nagy N, Ngan E, Obermayr F, Pachnis V, Pasricha PJ, Sham MH, Tam P, Vanden Berghe P. White paper on guidelines concerning enteric nervous system stem cell therapy for enteric neuropathies. Dev Biol 2016;417:229–251.
5. Heuckeroth RO. Hirschsprung disease: integrating basic science and clinical medicine to improve outcomes. Nat Rev Gastroenterol Hepatol 2018;15:152–167.
6. Clavé P, Shaker R. Dysphagia: current reality and scope of the problem. Nat Rev Gastroenterol Hepatol 2015;12:259–270.
7. Becker L, Mashimo H. Further promise of stem cells therapies in the enteric nervous system. Gastroenterology 2009;136:2055–2058.
8. Kulkarni S, Becker L, Pasricha PJ. Stem cell transplantation in neurodegenerative disorders of the gastrointestinal tract: future or fiction? Gut 2012;61:613–621.
9. Heanue TA, Pachnis V. Enteric nervous system development and Hirschsprung's disease: advances in genetic and stem cell studies. Nat Rev Neurosci 2007;8:466–479.
10. Gao F, Chiu SM, Motan DA, Zhang Z, Chen L, Ji HL, Tse HF, Fu QL, Lian Q. Mesenchymal stem cells and immunomodulation: current status and future prospects. Cell Death Dis 2016;7:e2062.
11. Auletta JJ, Bartholomew AM, Maziarz RT, Deans RJ, Miller RH, Lazarus HM, Cohen JA. The potential of mesenchymal stromal cells as a novel cellular therapy for multiple sclerosis. Immunotherapy 2012;4:529–547.
12. Tanna T, Sachan V. Mesenchymal stem cells: potential in treatment of neurodegenerative diseases. Curr Stem Cell Res Ther 2014;9:513–521.
13. Sousa BR, Parreira RC, Fonseca EA, Amaya MJ, Tonelli FM, Lacerda SM, Lalwani P, Santos AK, Gomes KN, Ulrich H, Kihara AH, Resende RR. Human adult stem cells from diverse origins: an overview from multiparametric immunophenotyping to clinical applications. Cytometry A 2014;85:43–77.
14. Farini A, Sitzia C, Erratico S, Meregalli M, Torrente Y. Clinical applications of mesenchymal stem cells in chronic diseases. Stem Cells Int 2014;2014:306573.
15. Si YL, Zhao YL, Hao HJ, Fu XB, Han WD. MSCs: biological characteristics, clinical applications and their outstanding concerns. Ageing Res Rev 2011;10:93–103.
16. Tse WT, Pendleton JD, Beyer WM, Egalka MC, Guinan EC. Suppression of allogeneic T-cell proliferation by human marrow stromal cells: implications in transplantation. Transplantation 2003;75:389–397.
17. Newman RE, Yoo D, LeRoux MA, Danilkovitch-Miagkova A. Treatment of inflammatory diseases with mesenchymal stem cells. Inflamm Allergy Drug Targets 2009;8:110–123.
18. Ren G, Zhang L, Zhao X, Xu G, Zhang Y, Roberts AI, Zhao RC, Shi Y. Mesenchymal stem cell-mediated immunosuppression occurs via concerted action of chemokines and nitric oxide. Cell Stem Cell 2008;2:141–150.
19. Lin R, Ding Z, Ma H, Shi H, Gao Y, Qian W, Shi W, Sun Z, Hou X, Li X. In vitro conditioned bone marrow-derived mesenchymal stem cells promote de novo functional enteric nerve regeneration, but not through direct-transdifferentiation. Stem Cells 2015;33:3545–3557.
20. Kulkarni S, Micci MA, Leser J, Shin C, Tang SC, Fu YY, Liu L, Li Q, Saha M, Li C, Enikolopov G, Becker L, Rakhilin N, Anderson M, Shen X, Dong X, Butte MJ, Song H, Southard-Smith EM, Kapur RP, Bogunovic M, Pasricha PJ. Adult enteric nervous system in health is maintained by a dynamic balance between neuronal apoptosis and neurogenesis. Proc Natl Acad Sci U S A 2017;114:E3709-e18.
21. Yarandi SS, Kulkarni S, Saha M, Sylvia KE, Sears CL, Pasricha PJ. Intestinal bacteria maintain adult enteric nervous system and nitrergic neurons via toll-like receptor 2-induced neurogenesis in mice. Gastroenterology 2020;159:200–213.e8.
22. Birbrair A, Wang ZM, Messi ML, Enikolopov GN, Delbono O. Nestin-GFP transgene reveals neural precursor cells in adult skeletal muscle. PloS One 2011;6:e16816.
23. Suárez-Rodríguez R, Belkind-Gerson J. Cultured nestin-positive cells from postnatal mouse small bowel differentiate ex vivo into neurons, glia, and smooth muscle. Stem Cells 2004;22:1373–1385.
24. Almond S, Lindley RM, Kenny SE, Connell MG, Edgar DH. Characterisation and transplantation of enteric nervous system progenitor cells. Gut 2007;56:489–496.
25. Wright CM, Schneider S, Smith-Edwards KM, Mafra F, Leembruggen AJL, Gonzalez MV, Kothakapa DR, Anderson JB, Maguire BA, Gao T, Missall TA, Howard MJ, Bornstein JC, Davis BM, Heuckeroth RO. scRNA-seq reveals new enteric nervous system roles for GDNF, NRTN, and TBX3. Cell Mol Gastroenterol Hepatol 2021;11:1548–1592.e1.

26. Enomoto H, Crawford PA, Gorodinsky A, Heuckeroth RO, Johnson EM Jr, Milbrandt J. RET signaling is essential for migration, axonal growth and axon guidance of developing sympathetic neurons. Development 2001;128:3963–3974.
27. Soret R, Schneider S, Bernas G, Christophers B, Souchkova O, Charrier B, Righini-Grunder F, Aspirot A, Landry M, Kembel SW, Faure C, Heuckeroth RO, Pilon N. Glial cell-derived neurotrophic factor induces enteric neurogenesis and improves colon structure and function in mouse models of Hirschsprung disease. Gastroenterology 2020;159:1824–1838.e17.
28. El-Nachef WN, Bronner ME. De novo enteric neurogenesis in post-embryonic zebrafish from Schwann cell precursors rather than resident cell types. Development 2020:147.
29. McCallum S, Obata Y, Fourli E, Boeing S, Peddie CJ, Xu Q, Horswell S, Kelsh RN, Collinson L, Wilkinson D, Pin C, Pachnis V, Heanue TA. Enteric glia as a source of neural progenitors in adult zebrafish. Elife 2020;9.
30. Liu MT, Kuan YH, Wang J, Hen R, Gershon MD. 5-HT4 receptor-mediated neuroprotection and neurogenesis in the enteric nervous system of adult mice. J Neurosci 2009;29:9683–9699.
31. Singh A, Dawson TM, Kulkarni S. Neurodegenerative disorders and gut-brain interactions. J Clin Invest 2021:131.
32. Virtanen H, Garton DR, Andressoo JO. Myenteric neurons do not replicate in small intestine under normal physiological conditions in adult mouse. Cell Mol Gastroenterol Hepatol 2022;14:27–34.
33. Hanani M, Ledder O, Yutkin V, Abu-Dalu R, Huang TY, Härtig W, Vannucchi MG, Faussone-Pellegrini MS. Regeneration of myenteric plexus in the mouse colon after experimental denervation with benzalkonium chloride. J Comp Neurol 2003;462:315–327.
34. Laranjeira C, Sandgren K, Kessaris N, Richardson W, Potocnik A, Vanden Berghe P, Pachnis V. Glial cells in the mouse enteric nervous system can undergo neurogenesis in response to injury. J Clin Invest 2011;121:3412–3424.
35. Robinson AM, Miller S, Payne N, Boyd R, Sakkal S, Nurgali K. Neuroprotective potential of mesenchymal stem cell-based therapy in acute stages of TNBS-induced colitis in guinea-pigs. PLoS One 2015;10:e0139023.
36. Burdon TJ, Paul A, Noiseux N, Prakash S, Shum-Tim D. Bone marrow stem cell derived paracrine factors for regenerative medicine: current perspectives and therapeutic potential. Bone Marrow Res 2011;2011:207326.
37. Skalnikova H, Motlik J, Gadher SJ, Kovarova H. Mapping of the secretome of primary isolates of mammalian cells, stem cells and derived cell lines. Proteomics 2011;11:691–708.
38. Bae KS, Park JB, Kim HS, Kim DS, Park DJ, Kang SJ. Neuron-like differentiation of bone marrow-derived mesenchymal stem cells. Yonsei Med J 2011;52:401–412.
39. Zeng R, Wang LW, Hu ZB, Guo WT, Wei JS, Lin H, Sun X, Chen LX, Yang LJ. Differentiation of human bone marrow mesenchymal stem cells into neuron-like cells in vitro. Spine 2011;36:997–1005.
40. Freedman MS, Bar-Or A, Atkins HL, Karussis D, Frassoni F, Lazarus H, Scolding N, Slavin S, Le Blanc K, Uccelli A. The therapeutic potential of mesenchymal stem cell transplantation as a treatment for multiple sclerosis: consensus report of the International MSCT Study Group. Mult Scler 2010;16:503–510.
41. Ohtaki H, Ylostalo JH, Foraker JE, Robinson AP, Reger RL, Shioda S, Prockop DJ. Stem/progenitor cells from bone marrow decrease neuronal death in global ischemia by modulation of inflammatory/immune responses. Proc Natl Acad Sci U S A 2008;105:14638–14643.
42. Marconi S, Bonaconsa M, Scambi I, Squintani GM, Rui W, Turano E, Ungaro D, D'Agostino S, Barbieri F, Angiari S, Farinazzo A, Constantin G, Del Carro U, Bonetti B, Mariotti R. Systemic treatment with adipose-derived mesenchymal stem cells ameliorates clinical and pathological features in the amyotrophic lateral sclerosis murine model. Neuroscience 2013;248:333–343.
43. Sidorova YA, Saarma M. Small molecules and peptides targeting glial cell line-derived neurotrophic factor receptors for the treatment of neurodegeneration. Int J Mol Sci 2020:21.
44. McKeown SJ, Mohsenipour M, Bergner AJ, Young HM, Stamp LA. Exposure to GDNF enhances the ability of enteric neural progenitors to generate an enteric nervous system. Stem Cell Reports 2017;8:476–488.
45. Chandrasekharan B, Anitha M, Blatt R, Shahnavaz N, Kooby D, Staley C, Mwangi S, Jones DP, Sitaraman SV, Srinivasan S. Colonic motor dysfunction in human diabetes is associated with enteric neuronal loss and increased oxidative stress. Neurogastroenterol Motil 2011;23:131–138, e26.
46. Sanders KM, Ward SM. Nitric oxide and its role as a non-adrenergic, non-cholinergic inhibitory neurotransmitter in the gastrointestinal tract. Br J Pharmacol 2019;176:212–227.
47. Osman AM, Zhou K, Zhu C, Blomgren K. Transplantation of enteric neural stem/progenitor cells into the irradiated young mouse hippocampus. Cell Transplant 2014;23:1657–1671.
48. Shi H, Qi C, Meng L, Yao H, Jiang C, Fan M, Zhang Q, Hou X, Lin R. Bone marrow-derived mesenchymal stem cells promote Helicobacter pylori-associated gastric cancer progression by secreting thrombospondin-2. Cell Prolif 2021;54:e13114.
49. Sütö G, Király A, Taché Y. Interleukin 1 beta inhibits gastric emptying in rats: mediation through prostaglandin and corticotropin-releasing factor. Gastroenterology 1994;106:1568–1575.


**Received December 16, 2021. Accepted October 26, 2022.**

**Correspondence**
Address correspondence to: Rong Lin, MD, PhD, Department of Gastroenterology, Union Hospital, Tongji Medical College, Huazhong University of Science and Technology, Wuhan 430022, China. e-mail: linrong@hust.edu.cn.

**Acknowledgements**
The authors thank all study participants, researchers, technicians, and administrative staff who contributed to this study.

### CRediT Authorship Contributions

Mengke Fan (Data curation: Lead; Formal analysis: Lead; Investigation: Equal; Methodology: Equal; Project administration: Equal; Resources: Equal; Software: Equal; Writing – original draft: Lead; Writing – review & editing: Lead)

Huiying Shi (Data curation: Equal; Writing – original draft: Equal; Writing – review & editing: Equal)

Hailing Yao (Data curation: Supporting; Formal analysis: Supporting; Methodology: Supporting; Software: Supporting; Validation: Supporting; Visualization: Supporting)

Weijun Wang (Resources: Supporting; Supervision: Supporting; Validation: Supporting; Visualization: Supporting)

Yurui Zhang (Data curation: Supporting; Formal analysis: Supporting; Software: Supporting; Validation: Supporting; Visualization: Supporting)

Chen Jiang (Data curation: Supporting; Investigation: Supporting; Methodology: Supporting; Project administration: Supporting)

Rong Lin (Conceptualization: Lead; Funding acquisition: Lead; Project administration: Lead; Supervision: Lead; Visualization: Lead; Writing – review & editing: Lead)

### Conflicts of interest

The authors disclose no conflicts.

### Funding

Supported by the National Natural Science Foundation of China (nos. 81974068 and 81770539). The funders had no role in the design of the study, data collection and analysis, interpretation of data, and in writing the manuscript.